Monitoring of solar spectral ultraviolet irradiance in Aosta, Italy

Ilias Fountoulakis[1], Henri Diémoz[1,2], Anna Maria Siani[3], Gregor Hülsen[4], Julian Gröbner[4]

[1]Aosta Valley Regional Environmental Protection Agency (ARPA), 11020 Saint-Christophe, Italy
[2]Institute of Atmospheric Sciences and Climate, National Research Council, 00185 Rome, Italy
5   [3]Physics Department, Sapienza Università di Roma, 00185 Rome, Italy
[4]WCC-UV, PMOD/WRC, Dorfstrasse 33, Davos Dorf, CH-7260, SWITZERLAND

Correspondence to: Ilias Fountoulakis (i.fountoulakis@arpa.vda.it)

Abstract. A Bentham DTMc300 spectrophotometer is deployed at the station of Aosta–Saint-Christophe, Italy, at the headquarters of the Regional Environmental Protection Agency (ARPA) and performs continuous high quality spectral
10   measurements of the solar ultraviolet (UV) irradiance since 2006. The measuring site is located in the North-western of the Alps, in a large valley floor at the altitude of 570 m a.s.l., surrounded by mountains. It is very significant to have accurate measurements in such a sensitive environment, since the complex terrain and the strongly variable meteo-climatic conditions typical of the Alps induce large spatial and temporal variability in the surface levels of the solar UV irradiance. The spectroradiometer is moreover used as a reference of a regional UV network, with additional stations located at different
15   altitudes (1640 and 3500 m a.s.l.) and environmental conditions (mountain and glacier). In the present study we discuss the procedures and the technical aspects which ensure the high quality of the measurements performed by the reference instrument, and subsequently of the entire network. In particular, we describe the procedures used to characterize the Bentham for its characteristics which affect the quality of the measurements. The used Quality Control/Quality Assurance (QA/QC) procedures are also discussed. We show that the good quality of the spectral measurements is further ensured by a
20   strong traceability chain to the world reference QASUME and a strict calibration protocol. Recently, the spectral UV dataset of Aosta–Saint-Christophe has been re-evaluated and homogenized. The final spectra consist one of the most accurate datasets globally. At wavelengths above 310 nm and for solar zenith angles below 75° the expanded uncertainty in the final dataset decreases with time, from 7% in 2006 to 4% in the present. The present study not only serves as the reference document for any future use of the data, but also provides useful information for experiments and novel techniques which
25   have been applied for the characterization of the instrument, and the QA/QC of the spectral UV measurements. Furthermore, the study clearly shows that maintaining a strong traceability chain to a reference instrument is critical for the good quality of the measurements. The studied spectral dataset is freely accessible at https://doi.org/10.5281/zenodo.3934324 (Fountoulakis et al., 2020).

1 Introduction

30   Although less than 10% of the overall solar electromagnetic radiation that reaches the Earth's surface is in the ultraviolet (UV), the particular band of the solar spectrum is very significant for life on Earth. Exposure to solar UV radiation is necessary for living organisms since it triggers a number of beneficial processes (Juzeniene and Moan, 2012;Webb and Engelsen, 2008). However, over-exposure is harmful for the humans and the ecosystems (Caldwell et al., 1998;Häder et al., 2007;Juzeniene et al., 2011;Lucas et al., 2019). Various living organisms including humans have been slowly adapted proper

35   sun-exposure behaviours through the centuries, depending on the levels of solar UV radiation at the place where they live (Jablonski and Chaplin, 2000). Fast changing climate conditions, changes in habits and attitudes of people, and the increase of human migration have meant that many people all over the globe are now exposed to more or to less solar UV radiation than in the past (Bornman et al., 2019;Cadario et al., 2015;Hintzpeter et al., 2008;Lips and de Jongh, 2018). Thus, continuous and accurate monitoring of the levels and the variability of the solar irradiance in the UV spectral region is

40   necessary for the accurate and on time detection of trends (Glandorf et al., 2005;Weatherhead et al., 1998), as well as estimating different exposure scenarios in order to inform the public and hence to better understand and clarify the balance between the risks and benefits of solar UV radiation under difference conditions (Blumthaler, 2018).

Ozone is the main absorber of the (more energetic) photons in the UV-B region, which are more effective on causing both acute (e.g. erythema) and chronic (e.g. DNA damage) problems relative to longer UV wavelengths. Anthropogenic

45   emissions of Ozone Depleting Substances (ODS) led to enhanced chemical destruction of stratospheric ozone over high latitudes of the North and the South hemisphere in spring in the 1980s, and subsequently to very high levels of UV-B irradiance at the Earth's surface relative to its past climatological levels (Solomon et al., 1986). The concern increased even more after ozone loss occurrences also experienced at middle latitudes which in turn affect solar UV levels at ground (Kerr and McElroy, 1993;Zerefos et al., 1995;Herman et al., 1996;Petkov et al., 2014). The apparent increase of UV-B irradiance

50   led to the development and deployment of a large number of instruments performing spectral or broad-band measurements of the UV-B irradiance, as well as quantities directly linked to biological effects of the UV radiation such as the ambient erythemal irradiance (Booth et al., 2013;Gröbner et al., 2006;Schmalwieser et al., 2017). Since the 1980s, improved spectral sensors have been developed, providing more accurate measurements in a wider range of wavelengths extending up to the visible region (e.g. De Mazière et al. (2018), Zuber et al. (2018)). Furthermore, many international and national inter-

55   comparison campaigns allowed the identification of the main factors introducing uncertainties in the measurements (Bais et al., 2001;Diémoz et al., 2011;Huelsen et al., 2020;McKenzie et al., 1993;Seckmeyer et al., 1994), and subsequently the improved characterization of the instruments, and further reduction of the uncertainties. The good quality of spectral UV measurements performed at different stations around the world is generally ensured by the adoption of standard calibration procedures and comparison with world reference standard instruments which have been developed for this purpose (Gröbner

60   et al., 2006).

The main sources of uncertainty in the spectral UV measurements have been discussed in the studies of Bais (1997) and Bernhard and Seckmeyer (1999). In both studies they conclude that uncertainties in the spectral UV measurements depend on the characteristics of the measuring instrument and the atmospheric conditions. An inter-comparison between nineteen different instruments in 1997 (Bais et al., 2001) showed that the agreement between well characterized and calibrated
65 instruments is 10% at wavelengths above 300 nm, which is indicative for the expanded uncertainty in the measurements. In a more recent study, Cordero et al. (2008) estimated the uncertainty in the measurements of a double monochromator Bentham spectrometer to 9% for wavelengths above 300 nm and SZAs smaller than 30°. Garane et al. (2006) estimated the expanded uncertainty in the measurements of two Brewer spectrophotometers, with a single and a double monochromator, to 13% and 10% respectively for SZAs below 75° and wavelengths below 305 nm. However, significant progress has been achieved in
70 the past two decades regarding the methods used for the instrument calibration and characterization, and the quality assurance and quality control (QA/QC) procedures (Fountoulakis et al., 2016;Fountoulakis et al., 2017;Gröbner et al., 2010;Hülsen et al., 2016;Lakkala et al., 2018;Lakkala et al., 2008), which in conjunction to the improvement of the technical characteristics of the instruments (Gröbner, 2003;Pulli et al., 2013) allows spectral measurements with expanded uncertainty of ~2% for wavelengths above 310 nm (Hülsen et al., 2016). Low uncertainty measurements are necessary for the detection
75 of trends in the levels of solar UV irradiance (Bernhard, 2011;Seckmeyer et al., 2009;Weatherhead et al., 1998). According to Glandorf et al. (2005) the magnitude of the detected trends has to be at least larger than the magnitude of the natural variability of the irradiance and the uncertainty in the measurements in order to consider the detected trends reliable.

In the context of the present study the methods described in the existing bibliography, as well as new methods have been used to characterize a Bentham DTMc300 spectrometer which performs spectral measurements in the UV and visible (VIS)
80 region of the solar spectrum. The instrument is located at the facilities of Aosta Valley Regional Environmental Protection Agency (ARPA VdA) at Saint-Christophe, Aosta, Italy. The strict QA/QC protocol and the strong traceability chain which ensure the good quality of the spectra are also discussed. Analysis and calculation of the overall uncertainty budget in the spectra, after re-evaluation and homogenization of the measurements certifies that the spectral UV record of Aosta is one of the most accurate datasets globally. Summarizing, the present document deals with the technical aspects of the instrument
85 and the dataset. Analysis and interpretation of the results, including the study of the long-term trends at the Aosta, Saint-Christophe site, will be addressed in a following study.

In Sect. 2 description of the site location and the technical characteristics of the instruments are provided. The instrument characterization techniques and the methods used for the QA/QC and the correction of the spectra are described in Sect. 3. The traceability chain is described in Sect. 4. In the same section the different versions of the data are discussed. The main
90 uncertainty sources and the overall uncertainty budget of the spectra are discussed in Sect. 5. Finally, in Sect. 6 the main findings of the study are summarized.

2 Location and instruments

2.1 Location

The Aosta Valley is an administrative region at the North of Italy. Since it is located in the North-western Alps, its altitude
reaches 4800 m a.s.l. (Mt Blanc), with an average of 2000 m a.s.l.. The valley floor where the main settlement (Aosta) is
located is surrounded by tall mountains, up to 3500 m a.s.l.. The rough terrain, the (spatially and temporally) varying surface
albedo and the very complex atmospheric conditions lead to surface levels of UV irradiance which may differ significantly,
not only in time but also in space, even within a horizontal distance of a few kilometres (Diémoz and Mayer, 2007). Thus,
satellite forecast and model estimates are uncertain over the region, especially under cloudy conditions (Diémoz et al.,
2013;Fountoulakis et al., 2019). Furthermore, high surface albedo and less dense atmosphere lead to extremely high levels of
the UV irradiance at the highest altitude regions of the Aosta Valley in spring and summer (Casale et al., 2015) and
correspondingly high exposure of the tourists and the locals to UV radiation (Siani et al., 2008). Also taking into account that
the levels of surface UV radiation are projected to change in the following decades as an adverse effect of climatic change in
the sensitive Alpine environment (Bais et al., 2015), it is easy to understand that continuous and accurate monitoring of the
solar UV irradiance is essential for the particular region. In order to cover this need, the UV monitoring network of the Aosta
Valley which is the first UV monitoring network in Italy, has been created. It includes instruments deployed at three sites at
different altitudes (Figure 1): Aosta – Saint-Christophe (45.7° N, 7.4° E, 570 m a.s.l.), La Thuile (45.7° N, 7.0° E, 1640 m
a.s.l.), and Plateau Rosa (45.9° N, 7.7° E, 3500 m a.s.l.). Although the horizontal distance between them is short (< 35 km),
the altitude range is large (3000 m) and they are located in quite different environments (valley bottom, mountain and
glacier).

The reference instrument of the network is the double monochromator Bentham DTMc 300 spectrometer with serial number
5541 (hereafter referred as Bentham5541) located at the Observatory of the Regional Environmental Protection Agency of
the Aosta Valley (ARPA VdA), at Aosta-Saint Christophe (hereafter the observatory is referred as AAO).
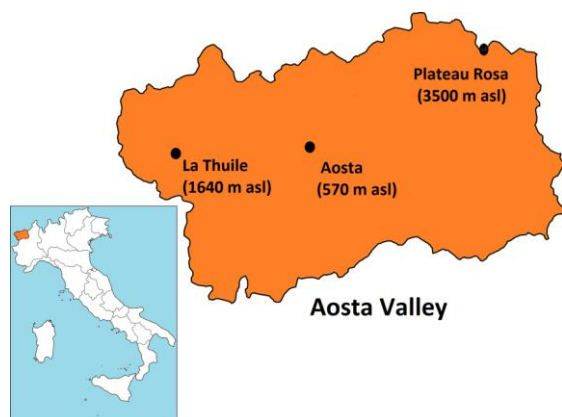
Figure 1: The stations of the UV monitoring network of the Aosta Valley

2.2 The Bentham spectroradiometer

In 2004, the Bentham5541 was deployed at the facilities of ARPA VdA and since that year it has been performing spectral measurements in the range 290 – 500 nm (Diémoz et al., 2011). In 2006, the first inter-comparison with the world reference QASUME (Gröbner and Sperfeld, 2005;Hülsen et al., 2016) was performed and allowed the detection of particular
120 operational problems, which were fixed within a few weeks after the inter-comparison. High quality spectral UV measurements are thus available since 2006, since a strict protocol for the maintenance and the calibration of the system has been adapted and a strong traceability chain is followed. Currently, Bentham5541 is the reference instrument of the UV monitoring network of the Aosta Valley and its absolute calibration is transferred on a yearly basis to the broadband radiometers which are deployed at the three different stations. In addition to being the reference instrument of the network,
125 the highly accurate UV dataset of the AAO is very useful for climatological studies, and the validation of UV estimates from satellites and radiative transfer models (Fountoulakis et al., 2019).

The Bentham DTMc300 is manufactured by Bentham Instruments Ltd (https://www.bentham.co.uk/), with headquarters at Reading, United Kingdom. The spectrometer consists from a pair of symmetrical Czerny Turner monochromators arranged for additive dispersion. The two spectrometers are enclosed in a shielded box wherein the temperature is stabilized to 21°C
130 and the relative humidity is kept low with the use of desiccant. Analysis of the internal temperature recordings showed that the temperature in the box wherein the spectrometer and the photon counting system are enclosed is homogeneous within 2°C, and that the temperature of the photon counting system is stabilized within less 0.5 °C throughout the year (while the ambient temperature usually ranges from about -5°C in winter to 25°C in summer). From 2006 until the summer of 2019 the relative humidity in the box varied between 10% in winter and 60% in summer. Improving the insulation of the box in the
135 summer of 2019 resulted to relative humidity below 40% during the whole year. Under usual operational conditions a middle slit with a 1 mm width is used between the two monochromators. The width of the other two (entrance and exit) slits is 0.74 mm. The resulting slit function is approximately triangular with a spectral resolution (FWHM) of 0.54 nm. With the particular setup, the instrument is practically not affected by stray light.

The wavelength range and the step of each spectral scan can be determined by the operator. The spectral scans of the solar
140 irradiance are routinely performed in the range 290 – 500 nm with a step of 0.25 nm and a frequency of 1 scan per 15 minutes. The duration of each scan can also change by adjusting the samples per reading (SPR) properly. The wavelength range, the duration, and the frequency of the scans change for example when broad-band radiometers are calibrated at the AAO (wavelength range of 290 – 400 nm, scan time of about 3 minutes, scan repeated without resting time between consecutive spectral scans). During inter-comparison campaigns the measurement settings may also change in order to
145 achieve synchronized measurements with the reference instrument.

Solar irradiance enters the instrument through a quartz diffuser which is covered by a UV-transmittable quartz dome, and is enclosed in a thermally stabilized case. The whole system (case, diffuser, dome, desiccant) is hereafter referred as the optical head (OH) of the instrument. The OH is the UV-J1002-REG system which was purchased by Schreder CMS (Lofererstrasse

32, 6322 Kirchbichl, Austria). The light entering the diffuser is driven into the spectrometer using an optical fiber. A heater
150 has been installed in the OH, which has been regulated in order to keep the temperature above 32°C. The photomultiplier
tube (PMT) is a DH-10 side window Bialkali, with a maximum sensitivity in the UV. An amplifier (267 programmable D.C.
amplifier) amplifies the signal by a factor ranging between 1 and 10 and the signal is finally recorded by a computer (PC).
More specifications regarding the standard characteristics of the spectrometer can be found in the web-page of the company
(https://www.bentham.co.uk/products/components/dtmc300-double-monochromator-39/).

2.3 Other UV monitoring instruments of the network

155

Since 2007 spectral UV measurements in the range 290 – 325 nm have been performed by the single monochromator MKIV
type Brewer with serial number 066 (Brewer#066), which measures the solar irradiance with a step and a resolution of ~0.5
nm. Brewer#066 was moved to AAO from the Environment Institute of the European Union-Joint Research Centre, Ispra
(45.8° N, 8.6° E, 240 m a.s.l.) in 2007. At the AAO, the UV-A and erythemal (CIE, 1999;Webb et al., 2011) irradiances
160 have been measured by a UVS-AE-T dual-band Kipp & Zonen radiometer since 2005. A second radiometer of the latter type
was installed at the high altitude station of Plateau Rosa in 2007 and measures the same radiometric quantities. One more
radiometer (Yankee UVB-1) at the station of La Thuile provides measurements of the erythemal irradiance since 2005. In
2019 the UVS-AE-T at Saint Christophe stopped working and has been replaced by a UV-E Kipp & Zonen radiometer.
Since 2006, the Bentham5541 is the reference for all broadband UV monitoring instruments of the network with the
165 exception of the Brewer#066. The Brewer#066 is calibrated independently every two years from International Ozone
Services Inc. (IOS) (https://www.io3.ca/) using a 1000W lamp which in turn is traceable to the National Institute of
Standards and Technology (NIST) (https://www.nist.gov/). Measurements of the total column and the profiles of different
atmospheric components are also available at the station (Diémoz et al., 2019a;Diémoz et al., 2014;Diémoz et al.,
2019b;Siani et al., 2018), and can be used in order to better understand how UV radiation interacts with the atmospheric
170 components in the complex environment of the Aosta Valley. Radiative transfer models are also employed to estimate the
solar UV irradiance in the whole domain of study, and to predict the UV Index for the following days. This informative
parameter is provided by a bulletin for the general public of the health risk of UV radiation exposure.

2.4 The world reference QASUME

As already discussed the Bentham5541 is traceable to world reference QASUME. QASUME is a transportable reference
175 spectroradiometer for measuring spectral solar ultraviolet irradiance. It has been developed in the context of the European
Commission-funded project Quality Assurance of Spectral Ultraviolet Measurements (QASUME), from which it took its
name, aiming at being the reference standard for instruments performing spectral UV measurements around Europe. The
World Radiation Center at the Physical Meteorological Observatory in Davos (PMOD-WRC) is responsible for the
maintenance and the continuous improvement of the system. Since 2002 it is the reference standard for many stations around
180 Europe. The spectrometer of QASUME is a commercially available Bentham DM-150 double monochromator. Initially the

entrance optic was a CMS-Schreder, Model UV-J1002, which since 2016 has been upgraded, and the Bentham D6 input optic is used. Optimization of characterization methodologies and implementation of the new optic have reduced the expended uncertainties of solar spectral UV irradiance measurements from 4.8% in 2005 to 2.0% in 2016 in the spectral region above 310 nm (Hülsen et al., 2016). More information about QASUME can be found in the referred bibliography
185   (Gröbner and Blumthaler, 2007;Gröbner et al., 2006;Gröbner et al., 2005;Gröbner and Sperfeld, 2005;Hülsen et al., 2016).

3 Instrument characterization and measurement correction

Since 2006, there have been efforts to determine the individual instrumental characteristics of the Bentham5541 and apply proper correction factors to the spectra in order to take into account the instrumental characteristics which can introduce biases or errors in the dataset. In many cases it is not possible to correct the measurements, and the remaining biases or errors
190   are taken into account in the calculation of the uncertainty budget of the dataset (see Sect. 5). The instrumental characteristics mostly affecting the measurements, as well as the procedure followed for the determination of their effects and the subsequent correction of the measurements is described below.

3.1 Dark current and amplification

The dark current (D) is measured at the beginning of each spectral scan and is generally of the order of ±0.1 pA. Although
195   there are dependencies of the dark signal from temperature and the level of the intensity of the incoming light, the magnitude of the dark signal does not practically change during the spectral scan under usual operational conditions. The recorded signal from the sources used for calibration is larger by three orders of magnitude or more relative to the dark signal for wavelengths above 280 nm. Thus, the uncertainties in the determination of the calibration factor related to the dark signal can be considered negligible. The role of dark signal may be more significant for very short wavelengths (shorter than 305
200   nm when SZA is larger than 75° or for smaller SZAs when the sky is overcast). At 305 nm the irradiance is higher than the dark signal by at least two orders of magnitude, even at SZAs around 85°. Thus, for wavelengths longer than 305 nm and for SZAs below 85° we can consider that the uncertainties related to the dark signal correction are negligible relative to the overall uncertainty budget of the measurements. The uncertainties related to the amplification (A) of the recorded signal (I_0) are also negligible. The corrected signal (I_1) at each wavelength is calculated from Eq. 1.
205

$$I_1 = (I_0/A) - D \quad (Eq.\,1)$$

3.2 Temperature of the Teflon diffuser

As discussed in the study of Ylianttila and Schreder (2005) the transmissivity of the Teflon diffuser to solar radiation changes with respect to temperature. The temperature of the Teflon diffuser is recorded using a thermistor which has been
210   installed in the OH and is in contact with the bottom surface of the diffuser. The temperature stabilization system can warm

up, but not cool down the diffuser. Thus, in summer the diffuser is getting warmed above the temperature stabilization point (32°C), and around local noon its temperature may reach 40°C. In winter, the temperature stabilization system cannot always fully compensate for the very low ambient temperatures. Thus, the temperature of the diffuser may be very low (~15°C) in the morning. Around noon (in winter) the temperature increases and is usually closer to the desired level. The response of

215 Teflon diffusers similar to that of Bentham5541, increases fast by 3% from 15°C to 22°C, and thereafter decreases gradually by 2% between 22°C and 45°C (Ylianttila and Schreder, 2005). The dependence from wavelength is very small and thus it is considered negligible and is not taken into account for the correction of the measurements. In particular, the signal I_1 calculated from Eq. 1 is corrected for the effect of temperature using Eq. 2:

220 $I_2 = I_1 / cf$ (Eq. 2)

Where, I_2 is the corrected signal, and cf is the correction factor. The correction factor is calculated from Eq. 3:

$y = a \cdot x + b$ (Eq. 3)

225

Where a and b depend from temperature of the diffuser θ. More specifically:
For θ<15°C, $a = -0.00075, b = 0.99675$
For θ>=15°C and θ<22°C, $a = 0.0043, b = 0.9104$
For θ>=22°C, $a = -0.00083, b = 0.9867$

230 The coefficients a and b were taken from Ylianttila and Schreder (2005). Before 2017, temperature was recorded at the beginning of each scan and no correction was applied to the spectra. Since the 125th Day of the Year (DOY), in May of 2017 the temperature is recorded several times during the spectral scan and all spectra are automatically corrected for the effect of temperature using Eq. 2. However, appropriate experiments were performed in order to ensure that the correction of the measurements is accurate.

235 In order to investigate if there is any dependence from temperature after applying the correction factors we performed two different tests. First, we performed measurements using 200 Watt lamps from early morning until late noon in a summer day, during which the temperature of the diffuser changed by 6°C (from 34°C to 40°C). After correction we could not detect any dependence from temperature.

In a different day we transferred the OH inside the optical laboratory and switched off the temperature stabilization system

240 of the Bentham's OH. We cooled the air in the room down to 18°C during the night and in the morning we begun performing measurements of the irradiance from different (1000 Watt and 200 Watt) lamps. The temperature stabilization system remained switched off and the air in the room was gradually warmed up while measurements were performed at different temperatures. A thermal camera was used to monitor the temperature of the diffuser complementary to the thermistor recordings. Before taking each picture with the camera, the dome that covers the diffuser was removed. When temperature

245   reached 28°C the stabilization system was turned on and used to increase the temperature of the diffuser up to 32°C. Then, an electrical heater was used in order to further increase the temperature in the room, and consequently the temperature of the diffuser, up to 41°C.
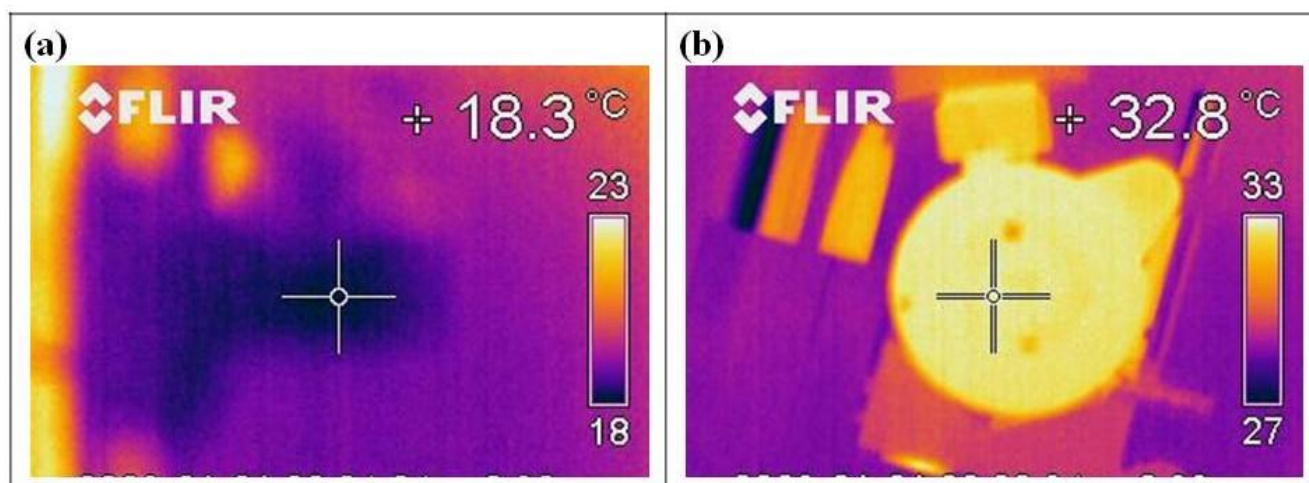
Figure 2: Temperature of the optical head (a) in the morning with the internal heating turned off, and (b) with the internal heating
250   **turned on.**

In Fig. 2, two different pictures taken with the thermal camera are presented. In both the homogeneity in the temperature of the OH is obvious. In all cases, the temperature recorded by the thermistor, and the temperature measured by the thermal camera agreed within 1°C.

Fountoulakis et al. (2017) showed that during measurements of the irradiance using 50 Watt lamps (distance between the
255   lamp filament and the diffuser was 5 cm) with a Brewer spectrophotometer, the temperature of the Teflon diffuser was inhomogeneous, and was higher by 5-6°C at the center relative to the edges of the diffuser. However, measurements with the thermal camera in Aosta showed that even when the extender of the calibrator (which increases the distance between the lamp filament and the diffuser from ~7 cm to ~20 cm) is not used during measurements of the irradiance from 200 Watt lamps, the temperature variations over the diffuser are below 2°C. The accuracy of the correction has been finally verified by
260   the fact that the agreement among the lamp spectra recorded at temperatures between 18°C and 41°C is better than 0.5% for wavelengths above 350 nm, and 1% for shorter wavelengths.

When the short setup (calibrator without the extender) of the calibrator is used, the diffuser is warmed up during measurements of the lamps' irradiance. In summer days temperatures up to 46°C have been recorded. Thus, since mid-2018 the extender has been used in order to increase the distance between the lamp and the diffuser to ~ 20 cm. Although using
265   the long setup results to increased noise because of the weaker signal (thus, slightly higher uncertainty in the retrieved calibration factors) the diffuser is not practically warmed during measurements.

3.3 Angular response

3.3.1 Characterization

Despite the progress that has been achieved regarding the improvement of the angular response of the Teflon diffusers

270   commonly used as entrance optics, there are still imperfections that induce uncertainties in the measurements, even when

high quality entrance optics are used (as in the case of Bentham5541). The angular response of the diffuser was measured at

the facilities of the PMOD-WRC in 2014 and is presented in Fig. 3. The characterization methodology was similar to that

described in the studies of Antón et al. (2008) and Bais et al. (1998).
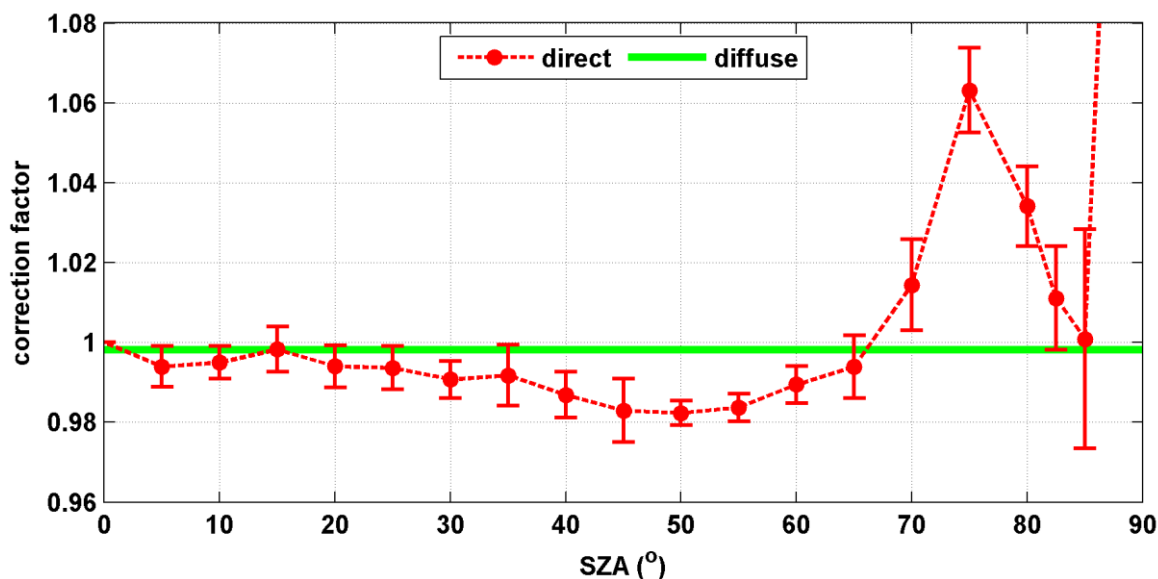
275   **Figure 3: Correction factors for the direct and diffuse components of the measured irradiance as a function of the SZA. Red dots represent the average correction factor (for all four azimuth directions) for the direct component. Error bars represent the corresponding standard deviation.**

The characterization was performed for SZAs 0 - 90° with a step of 5° at four different azimuth directions. These directions,

relative to the orientation of the diffuser during usual operational conditions, are North, South, West, and East. The

280   correction factor for the direct irradiance presented in Fig. 3 has been calculated as the ratio between the real and the ideal

angular response. The correction factor for the diffuse component is ~0.998 and has been calculated by assuming that the

diffuse irradiance is distributed uniformly in the horizon and integrating over the whole upper hemisphere (see e.g. Gröbner

et al. (1996)). For the direct component the error is less than 2% for SZAs below 70°, increases up to 6% at 75°, then

decreases again up to 85°, and increases fast thereafter. However, even in the visible range of the solar spectrum, the direct

285   component has a very small contribution to the overall solar irradiance at SZAs above 85° making the effect of the cosine

error at such large SZAs insignificant.

For the same SZAs, the correction factors at the four different directions differ to each other by less than 2% (±1% relative to the average) up to the SZA of 80°. The small differences which are within the uncertainty of the characterization show that the cosine response of the diffuser is practically independent from the azimuth direction. For SZAs between 80° and 88° the

290 differences between the responses at different planes gradually increase reaching a maximum of about ±5% relative to the average, at 88°. However, the characterization uncertainties above 80° are large due to the low signal and the finite width of the light beam used for the characterization, as well as the effect of errors in the direction of the incident light beam (at 88°, an error of 0.1° leads to a corresponding difference of 5% in the measured irradiance) which introduce additional uncertainties. Thus, (at least part of) the difference is again more likely due to the characterization uncertainties than real

295 differences in the response.

The angular response of Teflon diffusers similar as the one used for Bentham5541 is generally getting worse (thus the error is getting larger) with increasing wavelength. However, as shown in studies investigating the particular subject, differences become important for wavelengths longer than 500 nm. Characterization of similar diffusers in the range 300 – 500 nm yielded differences of the order of 2% or smaller (Bernhard and Petkov, 2019) .

300 **3.3.2 Modelling the errors**

The error in the measurements of global irradiance depends on the ratio between the direct and diffuse components (Bais et al., 1998). Thus, in order to estimate the error due to the non-ideal angular response of the instrument, simulations of the direct and the diffuse components were performed for SZAs between 0° and 90° using the model UVSPEC included in libRadtran package (Emde et al., 2016). Simulations were performed for typical columnar ozone of 320 DU, and AOD equal

305 to 0.05 and 0.2 (at 500 nm). AOD was scaled to shorter wavelengths using an Angstrom exponent equal to 1. A six-stream approximation was used for pseudospherical atmosphere and standard atmospheric profile (Anderson, 1986). We investigated the results for two different altitudes: 570m, and 1590 m. The former is the altitude of the AAO, while the latter is the altitude of the PMOD-WRC (46.8°N, 9.8°E, 1590 m a.s.l.). Simulations for Davos were performed in order to show that at such high altitudes the error becomes more important. These results are also useful for the discussion carried out in

310 the following sections since in July of 2014 the Bentham5541 took part in an inter-comparison campaign at Davos.
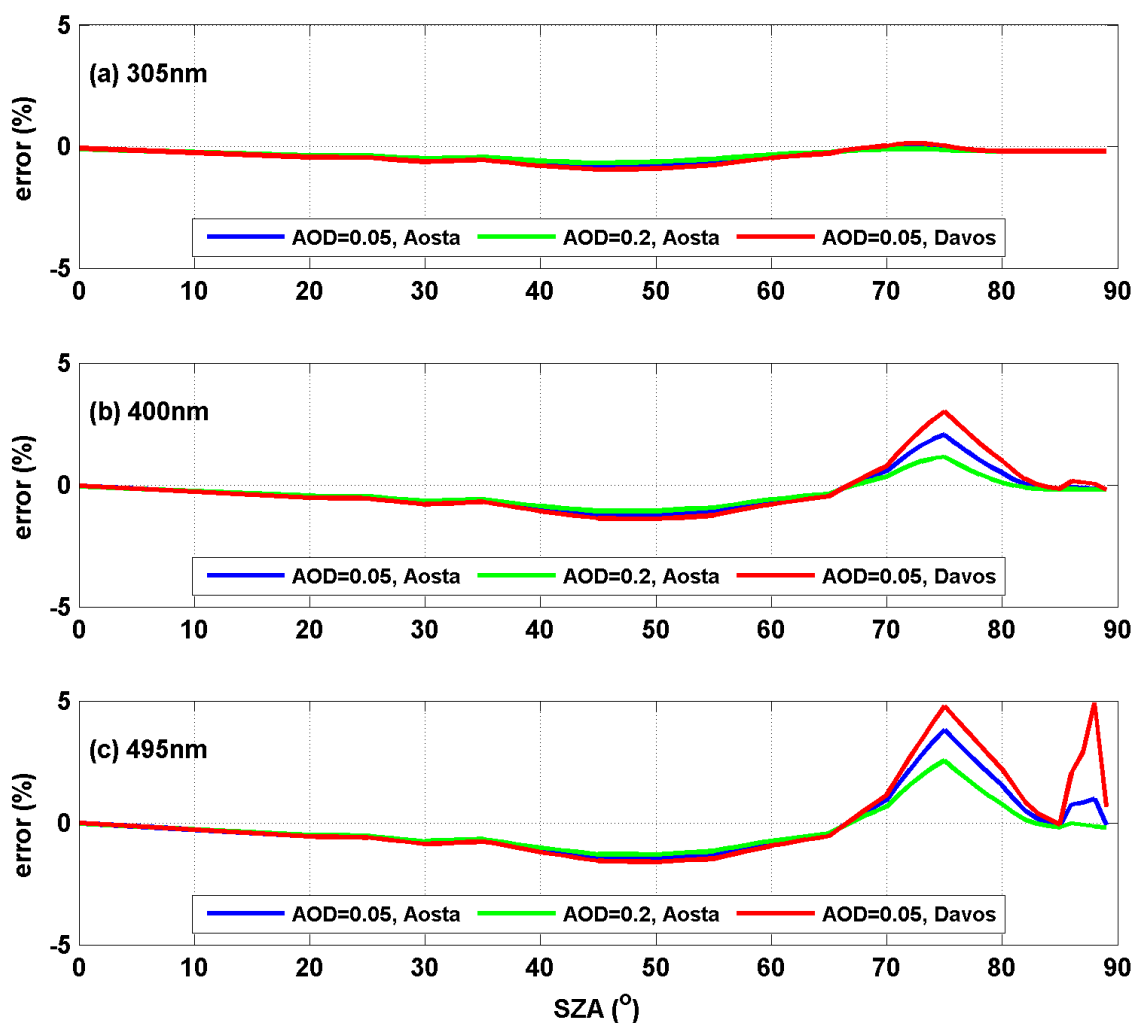
Figure 4: Modeled error in the measured irradiance for three different wavelengths: (a) 305 nm, (b) 400 nm, and (c) 495 nm. The results are for AAO (for AOD at 500 nm equal to 0.05 and 0.2) and the PMOD-WRC (for AOD at 500 nm equal to 0.05).

The results for 305, 400, and 495 nm and AOD at 500 nm equal to 0.05 and 0.2 (for Aosta), and 0.05 (for Davos) are

315   presented in Fig. 4. The results for AOD=0.2 are not presented for Davos since the particular value is unrealistic for that

station. For wavelengths below 350 nm the error remains always below 1% because at such short wavelengths the diffuse

component of the irradiance is dominant for SZA larger than 70° where the angular response is worse. For longer

wavelengths the errors become more important. For the SZA of 75° and 495 nm the error is 4% for Aosta and 5% for Davos

when AOD is 0.05. Taking into account the uncertainty in the characterization of the diffuser, and the fact that the cosine

320   response at 495 nm may be slightly worse than that measured at 320 nm we estimate that the maximum error may be slightly

larger, i.e. ~5% for Aosta and ~6% for Davos. For SZAs larger than 85° the contribution of the direct irradiance at Aosta is very small even for wavelengths near 500 nm, resulting to errors below 2%. However, at Davos the contribution of direct irradiance is still significant resulting to errors of the order of 5%.

325 Systematic, relatively accurate correction for the effect of non-ideal cosine response can be achieved only if the ratio between the direct and the diffuse solar irradiance that reach the diffuser is known. However, measurements of the direct component of spectral irradiance are not available. The use of a modelling approach as suggested by other studies (Lakkala et al., 2018) in order to calculate the ratio, would be also highly uncertain because of the varying cloud, albedo and aerosol conditions, which cannot be easily modelled. In order to reduce the uncertainty related to the imperfect cosine response of the diffuser, a new Teflon diffuser with improved angular characteristics is planned to replace the one which is currently 330 used.

3.4 Alignment of the optical fiber and levelling of the fore-optics

The light that enters the diffuser is transmitted to the spectrometer through the optical fiber. There are two metallic heads at the two ends of the fiber. The light passing through the Teflon diffuser enters the fiber through a small aperture on the first head and exits the fiber through a second aperture on the second head. The aperture at the exit has to be aligned with the 335 entrance of the monochromator so that the maximum possible light enters the two monochromators. However, non-optimal alignment of the head at the exit of the fiber is not a big problem since it is implicitly taken into account during the instrument absolute calibration.

Optimal alignment of the metallic head relative to the reference plane of the diffuser at the entrance optics is more important. Improper positioning may result to inhomogeneous response of the diffuser with respect to the zenith and/or the azimuth 340 angle of the sun. The errors are again more significant for longer wavelengths for which the direct component is stronger, i.e. for measurements in the UV-A and VIS regions. During inter-comparisons with QASUME, continuous measurements are performed while the OH of each instrument is rotated by 180° in order to detect possible azimuthal dependence of the response, which would show that there is a problem with the azimuth response, which in turn might be due to the imperfect alignment of the head of the fiber. Based on the results of the inter-comparisons with QASUME reference in the period 2006 345 - 2019, we estimate that the errors related to the misalignment of the fiber optics are usually bellow ±0.5%, but are higher in particular periods of a few months (up to 3.5% for VIS and 2% for UV) as discussed in Section 5.

The levelling of the fore-optics (i.e. the Teflon diffuser) is checked on a weekly basis. The levelling is accurate within ± 0.1° and the corresponding error is generally negligible with the exception of a particular period. From 2006 until 15 January of 2015 the diffuser was levelled using the bubble which is adjusted to the optical head. Thereafter a levelling jig is used. A 350 particular problem led to a larger mis-leveling of the diffuser and correspondingly to larger errors in the measurements in the period 07/07/2014 – 14/01/2015. In particular, the OH was disassembled and re-assembled before an inter-comparison campaign in Davos in 2014. After re-assembling the OH the position of the bubble on the optical head changed. Thereafter, using the bubble of the optical head to align the diffuser leads to a mis-levelling of +0.7±0.1° at an azimuth direction of

~340° (~20° from the south, towards the west). After begin using the levelling jig the particular problem has been solved.
355 Due to this problem the variability in the ratio of synchronous clear-sky measurements between QASUME and AAO was wavelength dependent, varying from ± 1% at shorter wavelengths to ± 4% near 500 nm during the 2014 inter-comparison campaign at Davos, which is unusually large.

3.5 Non-linearity

Before 24 July of 2006 the AAO measurements were performed with the high voltage (HV) of the PMT set to 670 V. In the
360 particular period measurements were suffering from significant non-linearity and the dependence of the response from the level of the measured signal was strong. Thus, the HV was thereafter lowered to 400 V. Although lowering the HV so much led to increased noise in the measurements, it also solved the issue of non-linearity, as has been confirmed after performing the experiments described below.

3.5.1 Linearity during usual operational conditions

365 The maximum photocurrent measured by Bentham5541 (in the noon of cloud free summer days) is of the order of ~300 nA. During the Davos inter-comparison campaign in 2014 the measured signal reached higher values of ~500 nA. It is noteworthy that before lowering the high voltage of the PMT (in July, 2006) the photocurrent was of the order of 15000 – 20000 nA. Two possible problems during the regular operation of similar instruments are the following:

1. The response may change after a few days of consecutive measurements
370 2. The response may change in the day following the intensity of the recorded signal.

In order to investigate the first issue, consecutive spectral scans, without leaving any rest time between them, were performed in the range 280 – 400 nm between 27 June 2018 and 6 July 2018. The sky during most of these days was cloudless and the levels of the UV irradiance were very high (noon UV index between 7 and 9). The irradiance of two 200 Watt lamps was measured at the beginning and at the end of the 10-day period, and for both lamps the difference was less
375 than 0.5%. The diffuser temperature during the measurements performed in the two different days was similar (33.5 - 35°C) ensuring that the effect of differences in temperature have not played any significant role.

In order to investigate the second issue, measurements with 200 Watt lamps were performed at early morning, noon, and late evening of different summer days. Again, the irradiance at local noon was very high in all days. The measurements were repeated using different schedules for the spectral scans (different spectral range and different resting times between the
380 spectral scans). In all cases, after correcting the measurements for the effect of temperature (of the Teflon diffuser) the differences were again less than 0.5%.

3.5.2 Linearity for extremely high signal levels

As a second step we tried to investigate if the response of the instrument changes for signal levels higher than usual. In order to achieve higher signal levels we performed measurements using wider (or totally removing) slits. Measurements were performed in the period 18 – 20 September 2018. Sky was cloudless during most of the day for all three days. We used two different setups:

Setup 1: Standard entrance slit (0.74 mm), standard intermediate slit (1.00 mm), no exit slit

Setup 2: All slits were removed (no entrance, intermediate or exit slit)

When the first setup was used the maximum photocurrent was ~1100 nA (~ double than the maximum photocurrent in Davos, ~3-4 times higher than maximum photocurrent in Aosta). In the morning no measurements were performed until ~8:00 LT. Then, the irradiance of two different 200 Watt lamps was measured. After performing the two scans, consecutive measurements of the solar irradiance in the range 290 – 400 nm were performed for ~3 hours (again without letting the PMT to rest between consecutive scans) using the same schedule as during QASUME inter-comparison campaigns. Then, spectral scans of the irradiance of the same two lamps were repeated (at ~13:30 LT). After correction for the effect of temperature the difference between the morning and noon lamp scans was again less than 0.5%. However, in this case the response of the AAO gradually increased while we were measuring the lamps irradiance at noon. The noon lamp scan lasted 40 mins, during which the response increased by ~0.5%. Since the increase is small and well below the instrumental uncertainties, we decided to perform one more experiment in order to further investigate if it is real.

Using the same (first) setup we continued performing spectral scans of the solar irradiance for ~ 1 more hour after finishing the lamp scans. After 1 hour of measurements we interrupted a spectral scan (at 370 nm when very strong signal had already been recorded) and within a few seconds we begun performing measurements of the irradiance from a 200 Watt lamp at 330 nm (photocurrent ~5nA). The lamp signal at the wavelength of 330 nm is weak, thus we assume that it does not affect the response of the PMT. Indeed, the response increased by ~0.5% in one hour after interrupting the spectral scans and remained relatively stable thereafter. In the first 40 minutes, the increase was 0.3 – 0.4% which confirms the findings of the first experiment.

In order to investigate if even higher signal has a stronger impact on the performance of the PMT we removed all slits and repeated the two experiments. The maximum photocurrent was ~2500 nA (~ 5 times higher than the maximum photocurrent in Davos, 9 – 10 times higher than maximum photocurrent in Aosta). In this case, the difference between the morning and the first noon scan of the irradiance from a 200 Watt lamp was ~3% (the response decreased by ~3% from morning until noon). Repeating the second experiment (interrupt spectral scans of the solar irradiance and perform continuous lamp measurements at a particular wavelength) resulted to increasing response (by ~2% in 100 minutes). In the 100 minutes of the measurements there was no sign of stabilization, showing that the response would probably keep increasing if the measurements had continued for more than 100 minutes.

According to these findings, the behaviour of the PMT can be considered linear for usual operational conditions, and even if
there is any non-linearity effect the relative uncertainty is much lower than the overall uncertainties in the measurements.

3.6 Wavelength shift

In order to correct the near real time spectra for the effect of wavelength shift, the SHICrivm algorithm (Slaper et al., 1995)
has been used, which results in a wavelength accuracy in the range 305 – 500 nm of the order of ±0.02 nm after correction.
The uncertainties in the processed spectra have been investigated and discussed in past studies (Diémoz et al., 2011;Gröbner
and Sperfeld, 2005) and are discussed in Sect. 5. Thus, no relative investigation has been performed in the context of the
present study. The re-evaluated spectra have been processed using the MATshic (Egli et al., 2016) instead of the SHICrivm
algorithm. However, the two algorithms are completely compatible when the same settings are used. Comparison between
spectra which have been processed using both algorithms also confirmed their compatibility.

3.7 Other issues

Between 2018 and 2020, there were five different periods of a few days (from 5 to 15) during which the Bentham5541 (for
different reasons) was not performing measurements of solar irradiance. Performing measurements with 200 and 1000 Watt
lamps during these periods showed that the response of the Bentham5541 gradually decreases (by 2-4% in a few days) and
then remains low as long as the instrument is inactive. Although it was not possible to detect the exact reasons that are
responsible for this change in the response, we noticed that the response returns to the pre-resting period levels directly after
setting back the instrument to regular operation and performing a few spectral scans. Thus, this issue was also not
investigated in more depth. Although the variability in relative humidity and temperature inside the shielded box which
contains the spectrometer may affect the electronic and mechanical parts of the instrument, it was not possible to detect any
clear correlation between the variability of the particular parameters and the response. In any case, performing the
calibrations on a monthly basis ensures that the response does not change by more than ~1.5% between consecutive
calibrations.

4 Calibration, traceability and data versioning

4.1 Traceability chain

Since the beginning of high quality spectral measurements in 2006, a strict protocol for the maintenance and the calibration
of the system has been adapted and a strong traceability chain has been followed. On a monthly basis, the Bentham5541 is
calibrated by measuring the irradiance from two 200 Watt (KS type, provided by Schreder CMS) lamps. The two lamps are
chosen from a set of three lamps. In the period 2006 – 2016 two of the 200 Watt lamps were sent on a yearly basis at the
facilities of the PMOD- WRC, where their spectral irradiances were measured. The type of the fore-optics of Bentham5541
and QASUME was the same in the particular period allowing the characterization of the full calibration setup used in Aosta

(measurements in Davos were performed using the calibrator of AAO). After the return of the lamps from Davos, they were
445   used as reference in order to re-calibrate the third 200 Watt lamp (which had not travelled to Davos) at the AAO. After
upgrading the fore-optic of QASUME in 2016 a direct calibration transfer of the 200 Watt lamps using the portable field
calibrator at Davos is impossible. Thus, a new optical laboratory has been set up at the AAO in 2018 and two new 1000 Watt
FEL lamps have been purchased, and are currently used as reference in order to re-calibrate the three working standard 200
Watt lamps. The two 1000 Watt FEL lamps are again shipped to PMOD – WRC on a yearly basis in order to be recalibrated.
450   Then, the spectral irradiance of each of the 200 Watt lamps is measured in the optical laboratory against the 1000 Watt
lamps. Regular inter-comparisons with the QASUME reference every one or two years complement and close the
traceability chain. The Bentham5541 is finally used as a reference instrument for the broad-band radiometers of the UV
monitoring network of the Aosta Valley. Side by side measurements are performed by Bentham and radiometers for 1-3
weeks (depending on the weather conditions) in order to transfer the calibration from the former to the latter.

455   The two different traceability chains for the periods 2006 – 2018 and 2018 – present are presented graphically in Fig. 5.
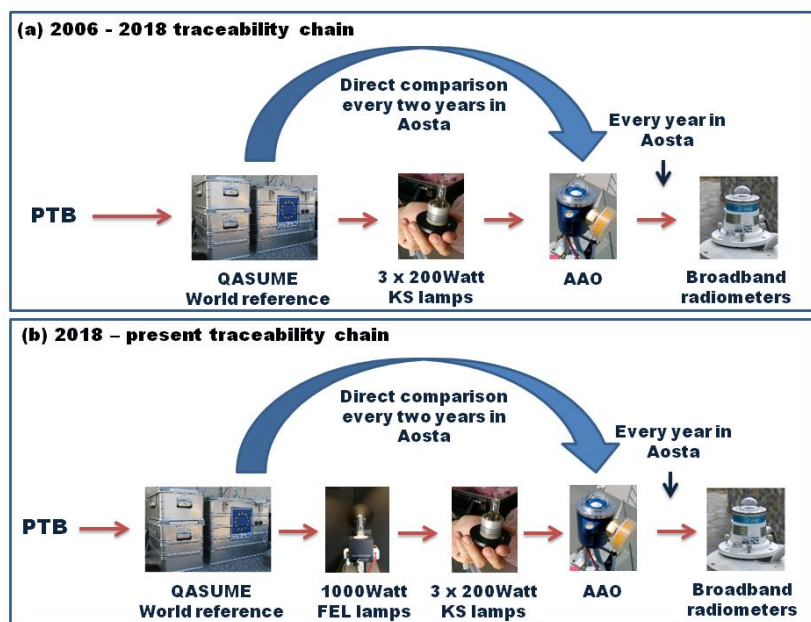
Figure 5: Traceability chain for (a) 2006 – 2018 and (b) 2018 – present

4.2 Re-evaluation and data versioning

We defined four available levels of measurements from the Bentham5541.

460   • **Level 0:** Raw photocurrent data
• **Level 1:** Near real-time irradiance spectra
• **Level 1.5:** Re-evaluated irradiance spectra
• **Level 2:** Re-evaluated irradiance spectra between two subsequent QASUME inter-comparisons

A more detailed description of each level of the data from AAO is provided in the following.

4.2.1 Level 0

The recorded signal during spectral scans of the solar (or lamp) irradiance is stored in ASCII files in units of electrical intensity (nA). Before being saved, the measurements have been corrected for the effect of dark signal. They have also been divided with the used level of amplification. The dark signal, the level of amplification, and the temperature of the diffuser are also saved in the same ASCII files. We consider the information in these ASCII files as the Level 0 data.

4.2.2 Level 1

Directly after measuring the irradiance from the 200 Watt lamps, the response of the instrument is calculated from each lamp following the methodology described in Bernhard and Seckmeyer (1999). If the difference between the responses from the two lamps is larger than 1%, measurements are repeated, and the reason that caused the difference is investigated. The lamp current is stabilized by a feedback-loop controlled circuit using a precision resistor and voltage, both calibrated once a year. The voltage across the lamp is monitored and recorded during measurements. The response calculated as the average response from the acceptable lamp scans is the Level 1 response which is thereafter automatically applied on spectral measurements. The recorded spectra are processed using the SHICrivm algorithm, and in near real time the information is stored in the database and after further processing (also performed in near real time) it is uploaded on the ARPA VdA web-page (http://www.arpa.vda.it/it/agenti-fisici/radiazione-solare/misure-uv-diretta). After DOY 125 of 2017 all measurements are also automatically corrected for the effect of temperature on the transmittance of the Teflon diffuser

The following information is produced by further processing the spectra and is then uploaded on the web-page:

- The UV-A irradiance (calculated by integrating measurements in the range 320 – 400 nm)
- The UV index (calculated by weighting measurements in the range 290 – 400 nm with the erythemal effective spectrum (CIE, 1999) and then integrating in the range 290 – 400 nm)
- Total ozone, calculated using a methodology similar to the methodology described in Bernhard et al. (2003).

On the web-page the particular quantities are directly compared with the corresponding quantities from other sources (measurements from collocated instruments, model and satellite estimates). The UV index is measured by Brewer#066 and the dual-band Kipp & Zonen radiometer, and the UV-A irradiance by the latter. Furthermore, on a daily basis, simulations of the clear-sky spectral irradiance in the range 290 – 400 nm are performed using the radiative transfer model UVSPEC of the libRadtran package (Mayer and Kylling, 2005). For the model simulations, the atmosphere is considered to contain a constant amount of continental aerosol. The total ozone used as input for the model is the forecast provided by the German Meteorological Service (DWD) for that day. A more detailed description of the model settings is provided in Diémoz et al. (2013). The clear-sky UV index and the UV-A irradiance are again calculated from the model spectra. Finally, the UV index and the UV-A irradiance from Bentham and all the above sources are compared to each other. Total ozone from the

495 Bentham5541 is compared with the total ozone from the Brewer#066 and satellite retrievals from the Ozone Monitoring
Instrument (OMI) on board Aura satellite (Levelt et al., 2018).

This way, both, the operators and the users of the web-page, can control the validity of the presented information. Large
differences among the instruments and/or extremely high/low values relative to the modelled irradiances may imply
operational problems of one of the instruments. On a daily basis un-expected results are investigated, and erroneous
500 measurements are directly removed from the database. The Level 1 dataset consists from the spectra and the response files
described above.

4.2.3 Level 1.5

The Level 1 dataset is inhomogeneous. For example, although the diffuser temperature is recorded at the beginning of each
scan, the spectra before the DOY 125 of 2017 are not corrected for the effect of temperature on the transmittance of the
505 Teflon diffuser, while a correction has been applied thereafter. The level 1.5 dataset has been homogenized by post-
correcting the whole Level 1 dataset for this effect. The changes are discussed in more detail below.

All spectra have been post-corrected for the effect of temperature. In addition to the solar spectra, temperature correction has
been applied on all lamp measurements (i.e. all calibration spectra). In Fig. 6, the ratio between the Level 1.5 and Level 1
irradiance at 305 nm and 495 nm is presented for the period 2010 – 2012, during which no other correction has been applied
510 to the measurements. The maximum differences resulting from the correction for the effect of temperature are of the order of
3% and the dependence from wavelength is small as can be perceived by Fig. 6. What is also obvious is that there is a clear
annual cycle in the variability of the ratio. The effect of temperature is more significant in winter and less significant in the
summer.
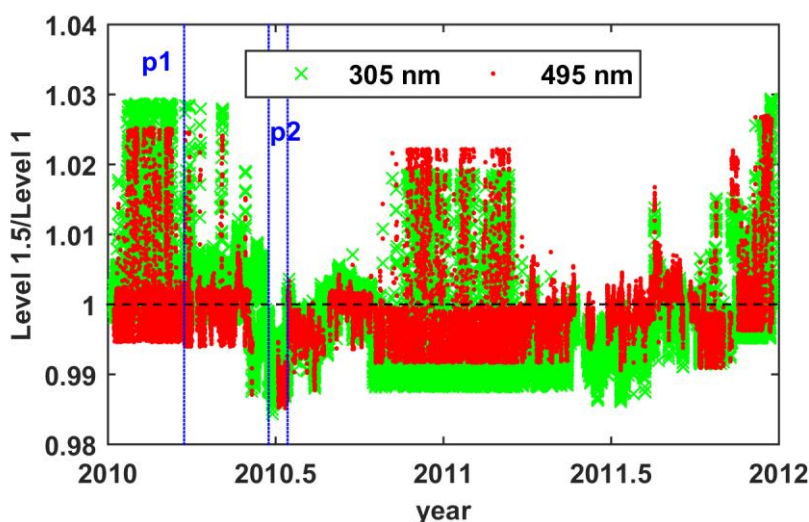
Figure 6: Ratio between the Level 1.5 and the Level 1 irradiances, at 305 nm (green x) and 495 nm (red dots). Two different periods have been marked on the graph in order to assist further discussion: p1 at the beginning of 2010 and p2 at mid-2010. The two wavelengths refer to the average of a band, over ±5 nm around the central wavelength.

The lowest values of the ratio at the beginning of 2010 (p1) are ~1.5% higher relative to the lowest values of the ratio in the period p2 (mid-2010 among blue dotted lines). This is because the temperature of the Teflon diffuser during the calibration in the first case was between 30°C and 33°C. In the second case the temperature was between 36°C and 42°C. Thus, applying the correction for the effect of temperature resulted to a larger change for p2.

The very large ratios (~1.03) in p1 are due to the correspondingly large variability in the temperature of the diffuser (from ~15°C to ~32°C) in winter. The flat "top" in Fig. 6 corresponds to the minimum response of the diffuser (for the range of recorded temperatures) at 15°C. The lowest values of the ratio do not go below a certain limit, again because the response becomes maximal at 22°C. The difference of ~ 0.5% between the results for 305 nm and 495 nm is mainly because of the warming of the diffuser by the lamps during calibration resulting to temperature increase of 2-3°C from the beginning until the end of the scan. Since 2017 the temperature is monitored with a step of 10 nm in the scan and the recorded values are used to correct the measurements. In order to take into account this effect for the period before 2017, an interpolation of the temperature values between consecutive scans is applied. When this is not possible, the value recorded at the beginning of the scan is used for the correction of all measurements in the scan.

4.2.4 Level 2

There are cases for which problems in the calibration procedure or the measurements have been detected a long time (of even months or years) after the data was stored in the database and uploaded on the web-page. Post-correcting the spectra for the above problems induces differences which in all cases are below 5%. Thus, we can consider that the Level 1 spectra can be safely used for informing the public without being misleading, and even the Level 1.5 spectra are of good quality. However, changes of the order of 5% in the dataset may induce non-negligible differences or biases in the climatological analysis of the data. Thus, the whole calibration dataset has been recently re-evaluated on the basis of the current level of knowledge. The results of the inter-comparisons with QASUME have been used to certify that the applied corrections have improved the accuracy of the dataset. Thus, only spectra between consecutive QASUME inter-comparisons are characterized as Level 2 spectra.

In Fig. 7, the ratio between the Level 2 and the Level 1 calibration factors at 310 nm, 400 nm, and 490 nm is presented for the period 2006 – 2019.
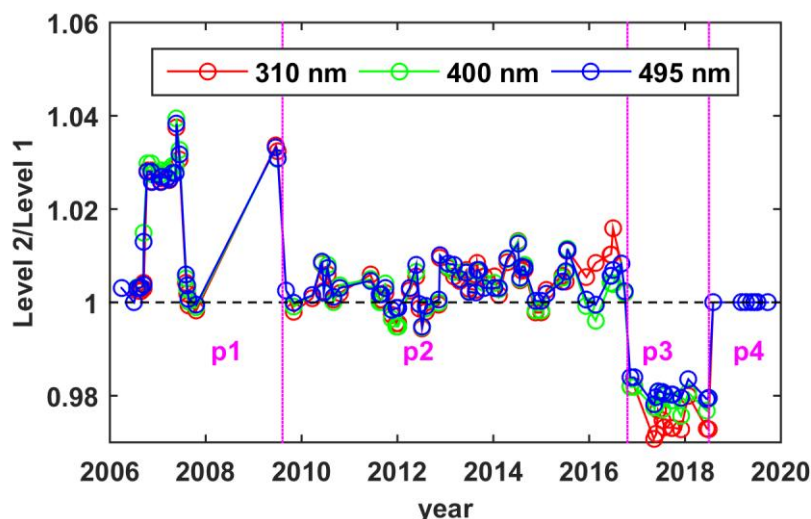
Figure 7: Ratio between the Level 2 and Level 1 calibration factors. Five different periods have been marked on the graph in order to assist further discussion: p1 from 2006 until 2009.6, p2 from 2009.6 until 2016.8, p3 from 2016.8 until 2018.5, and p4 from 2018.5 to 2020.

In p2 the only difference between the Level 2 and the Level 1 calibration factors, is the correction of the former for the effect of temperature. In most cases the temperature during calibration was above 28°C and the correction increased the response. Even in extreme cases the correction does not however exceed 2%. Larger differences of the order of 3 – 4% are evident in p1 and p3. More specifically, the Level 2 response is in many cases higher by up to 3 – 4% in p1 and lower by 2 – 3% in p3. It is obvious that not correcting the spectra would introduce a positive bias of the order of 2 – 3% if trends were calculated for the whole period. Analytical explanation of the causes of the differences in the used calibration factors is provided below. In March 2006, the first 200 Watt, type KS lamp with serial number 008 (KS008) was bought. Since then this lamp was used to calibrate the Bentham. The irradiance of KS008 was provided by the company as part of its quality certificate. From March until September 2006 the irradiance from the certificate has been used for the calculation of the response for both, Level 1 and Level 2. For that period, differences between Level 1 and Level 2 are small and mainly because of the correction for the effect of temperature.

In September 2006, the KS008 lamp was calibrated by PMOD-WRC at Davos. The calibration was performed using the portable field calibrator (PFC) of PMOD-WRC, and not that of AAO. The new certificate was used from 22 September 2006 until 10 August 2009 in order to calculate the response for the Level 1 dataset. During that period, two more 200 Watt lamps (KS023 and KS024) were purchased and calibrated in Aosta using KS008 as reference. During the 2007 inter-comparison with QASUME the AAO was calibrated using the lamps and the calibrator of PMOD-WRC and a difference of ~2% from the used response was found. Thus, all Level 1 calibration factors were thereon increased by ~2%. At the end of 2007 the lamps KS023 and KS024 were re-calibrated at the facilities of PMOD-WRC and the correction of ~2% stopped being applied. However, in August of 2009 it was found that there was a ~2.3% overestimation of the irradiances measured at

Davos (with a small dependence from wavelength) because of the use of the calibrator of PMOD-WRC instead of that of AAO. Since then, the lamps were shipped to Davos together with the PFC of AAO and the particular problem was solved. Applying that correction on the Level 2 calibration factors increased the responses for the period September 2006 – August 2009 by ~2.3%, with the exception of the period between the 2007 QASUME inter-comparison and the end of 2007, for

570 which the correction already applied in the Level 1 calibration factors was similar to that applied to the Level 2 correction factors. It should be noted that at the end of 2007 the magnetothermic switch of the Bentham5541 was broken and the system was stopped for several months. Thus measurements are not available during the entire year in 2008.

When KS008 was calibrated at Davos in 2006, the irradiance was overestimated by ~1% due to the then unknown reference plane of QASUME (Gröbner and Blumthaler, 2007) . Thus, the irradiances of KS008, KS023 and KS024 for the period 2006

575 – 2007 were additionally lowered by 1% (the responses have been increased by 1%). The overall increase in the Level 2 (relative to the Level 1) responses for September 2006 – August 2007 is ~3.3%. For the period August 2007 – December 2007, the increase due to the changes in the lamp irradiances is ~1.3% for the reasons explained above. For the beginning of 2009 the increase due to the changes applied to the lamp irradiances is ~2.3% since the reference plane of QASUME considered for the lamp calibration of 2007 was correct. However, correction for the effect of temperature increases the

580 variability in the ratio for the particular period.

Replacement of the fore-optics of QASUME in 2016 does not allow the calibration of the 200 Watt lamps at Davos anymore. The last calibration of 200 Watt lamps at the facilities of PMOD-WRC was thus performed in 2016. Re-evaluation of the calibration record showed that there was a problem with the irradiances measured in 2016 at Davos. Results of the 2017 inter-comparison with QASUME and the inter-comparison of broad-band radiometers held in Davos in 2018 (Huelsen

585 et al., 2020) , as well as characterization in the new optical laboratory at AAO in 2018 confirm that the real irradiances are possibly 2- 4% higher than those measured in 2016. A possible explanation could be that something changed in the PFC (e.g. during shipment of the PFC in 2016 from Davos to Aosta, or after disassembling and reassembling the PFC). Characterization of the 200 Watt lamps in the optical laboratory in 2018 showed a difference of ~2.5% between the calculated and the used irradiances for all lamps. The accuracy of the new irradiances (calculated in mid 2018) was also

590 confirmed during the 2019 inter-comparison with QASUME. Based on this result, the irradiances (and subsequently all calibration factors) in p3 have been corrected, leading to a ratio of 0.97 – 0.98 (also depending on the applied correction for the effect of temperature) between the Level 2 and the Level 1 responses. Since July 2018 (p4) no other changes have been applied on the used calibration factors and the ratio is constantly 1.

4.2.5 Data storage

595 Each Level 1.5 and Level 2 spectrum is saved in the database in the form of a NetCDF file together with all metadata which are necessary for the production of the Level 2 spectra from the raw data (i.e. dark current, diffuser temperature, spectra before the correction for wavelength shifts, spectral response etc), as well as the estimated uncertainty at each wavelength. The NetCDF file is structured according to the version 1.8 of the Climate and Forecast (CF) metadata conventions (Eaton et

al., 2020). In the same file the following effective doses which have been calculated from the particular spectrum are also
600   stored:

- Erythemal irradiance (CIE, 1999)

- Effective dose for the production of vitamin D (Bouillon et al., 2006)

- Effective dose for DNA damage (Setlow, 1974)

- Effective dose for plant damage (Caldwell, 1971)

605 - Effective dose for plant growth (Caldwell, 1971)

- Integrals of UV-B, UV-A and total UV irradiance

4.2.6 Inter-comparisons with QASUME

Analytical results of the inter-comparisons with QASUME between 2006 and 2019 are available on the web-page of PMOD-
610   WRC (https://www.pmodwrc.ch/wcc_uv/qasume_audit/reports/). The only exception is the 2014 inter-comparison held in
Davos for which the results are not publicly available. In Fig. 8, the average ratio between the measurements of the two
instruments at 310 nm (± 5 nm average), 390 nm (± 5 nm average), and 490 nm (± 5 nm average), as well as the
corresponding intervals of the 5/95 percentiles are presented. Shaded grey areas represent the combined expanded
uncertainty of the Bentham5541 Level 2 and the QASUME spectra for each intercomparison. The Bentham5541
615   uncertainties are reported and analytically discussed in Sect. 5. The two fold uncertainties of the spectra measured by
QASUME during intercomparisons are: 4.6% for 2006 – 2013, 2.9% for 2014 – 2017, and 1.9% for 2019 (Huelsen et al.,
2020;Hülsen et al., 2016). These numbers, as well as the uncertainties of Bentham5541 which have been used in order to
calculate the combined uncertainty are for SZAs below 75° and wavelengths longer than 310 nm. The uncertainties of the
two instruments are not completely independent since the same irradiance reference is used for the calibration of both. Thus,
620   the uncertainty in the calibration of the reference 1000 Watt lamps (used by PMOD-WRC to transfer the calibration to the
working standard lamps of both institutes) has not been taken into account when the overall radiometric uncertainty of
Bentham5541 was calculated. The presented ratios are for all SZAs. Both, the original (between the Level 1 and the
QASUME spectra) and the re-evaluated (between the Level 2 and the QASUME spectra) ratios are presented. It should be
noted at this point that in some cases the results in the PMOD-WRC reports differ from those for Level 1 spectra because a
625   re-evaluation was performed directly after particular campaigns.
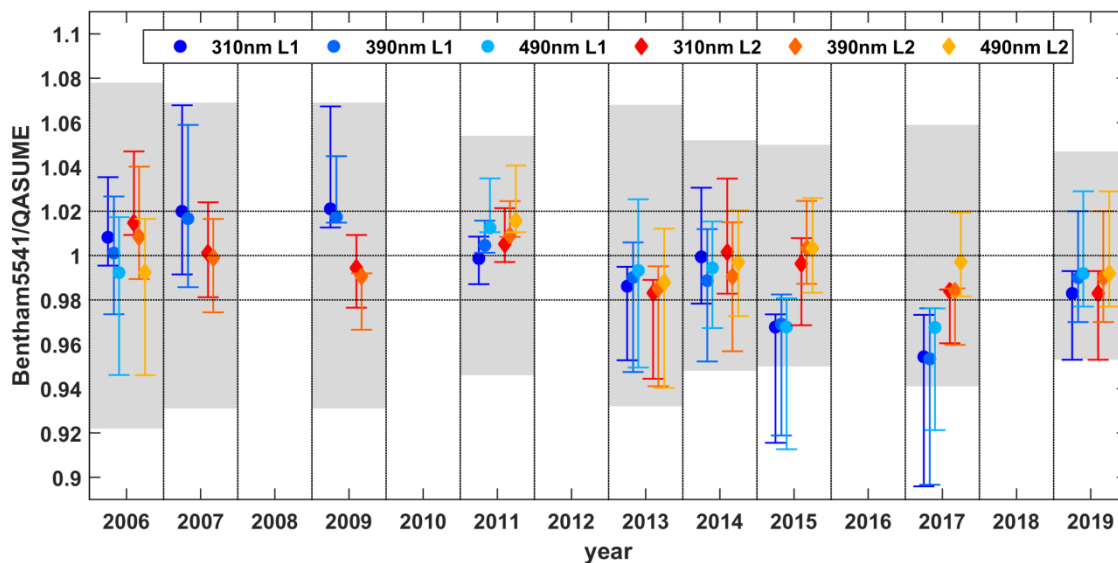
Figure 8: Average ratio between the measurements of Bentham5541 and QASUME at 310 nm, 390 nm, and 490 nm, and the corresponding 5/95 percentiles. Shaded area represents ±2% from perfect agreement between Bentham5541 and QASUME.

The general conclusions coming from Fig. 8 can be summarized as follows:

630 • There is a clear improvement of the results when the Level 2 dataset is used. The average ratio between Level 1 Bentham5541 and QASUME spectra ranges from -4% to +2%, while the average ratio between the Level 2 Bentham5541 and the QASUME spectra is always within ±2%.

• In all cases, the limits of the 5/95 percentiles for the Level 2 to QASUME ratio are within ±6%. This is because of the relatively larger differences between the two instruments for SZAs between 80° and 90°. If we exclude SZAs

635 above 75° from the analysis, then the limits are within ±4%. However, in both cases they are within the limits of the two fold combined expanded uncertainties.

• The 5/95 percentile intervals become narrower in some cases (e.g. 2007, 2009, 2015, 2019) for the Level 2 spectra. This is either because the used calibration factor changed for some of the days of the campaign (i.e. the same response is used for the whole period of the campaign instead of different responses for different days), or because

640 problematic spectra were removed from the dataset.

• With the exception of 2006, the dependence of the ratio from wavelength is small (less than 1%) for both, Level 1 and Level 2.

The remaining differences between the Level 2 and QASUME spectra have been in all cases explained; this way we were able to further quantify the effect of the factors that cause them on the Bentham5541 measurements.

645 • The dependence of the ratio from wavelength, as well as the large variability in **2006**, are due to the imperfect positioning of the fiber in the OH which induced a dependence of the ratio from the position of the sun.

• The differences between the Level 1 and Level 2 ratios in **2007** and **2009** are due to the changes in the used lamp irradiances, described in Sect. 4.2.4.

- The average difference of ~2% between AAO and QASUME in **2013** is again because of the non-optimal positioning of the fiber in the OH. The position of the fiber optics in the OH was optimized in 2007 and 2014, after detecting problems in 2006 and 2013 respectively.
- The **2014** inter-comparison took place in Davos and not in Aosta. As already discussed, small mis-leveling of the diffuser in the particular period affected the measurements and resulted to increased variability in the ratio (relative to the campaigns in 2013 and 2015).
- The average difference of ~2% between Bentham5541 and QASUME in **2017** and **2019** is because the fore-optics of QASUME was upgraded in 2016, and since then its angular response is better than the angular response of Bentham5541. A diffuser with improved angular characteristics will replace the one used by Bentham5541 in order to solve this issue.

In all cases the detected problems have been taken into account in the calculation of the overall uncertainty budget. A comprehensive discussion about the calculation of the overall uncertainty budget for different periods is provided in the following section.

5 Uncertainties

Diémoz et al. (2011) have already estimated the overall uncertainty in the Level 1 spectral measurements of the Bentham5541 based on the methods described in Gröbner and Sperfeld (2005) , Bernhard and Seckmeyer (1999) , and the Guide to the expression of Uncertainty in Measurement (BIPM et al., 2008). In this study the uncertainties reported by Diémoz et al. (2011) have been updated for the Level 2 spectra, as well as integrated quantities such as the UV-A and the erythemal irradiance. The overall uncertainty budget is not standard throughout the years since different problems affect measurements in different sub-periods. In the following, the word uncertainty denotes the standard (one fold) uncertainty unless something else is specified.

5.1 Radiometric uncertainty

Uncertainties in the calibration procedure play a very important role in the overall uncertainty budget. The main factors that are responsible for these uncertainties are discussed in the following.

5.1.1 Lamp certificate

When a lamp is characterized in an accredited laboratory, an uncertainty budget is specified for the lamp irradiance at each wavelength. The uncertainty budget generally depends on the individual characteristics of the lamp and the characterization procedure. The standard uncertainty reported in the lamp certificates until 2010 was 2.3% for all wavelengths. Since 2011 the reported uncertainties have been smaller and wavelength dependent. The uncertainty reported in the certificates of the 200 Watt and 1000 Watt lamps between 2011 and 2019 decreases with wavelength, ranging from 0.9 – 1.4% at 300 nm to 0.5 – 0.7% at 500 nm. When the lamps which have been calibrated to the accredited laboratory return to AAO, they are used

as references in order to recalibrate other lamps. An uncertainty budget has been also calculated for the lamps which are calibrated at the AAO.

5.1.2 Calibration transfer

The uncertainty due to the transfer of the calibration from the reference to the working standard lamps has not been taken
685 into account by Diémoz et al. (2011). In the study of Kazadzis et al. (2005) the uncertainty due to the transfer of the calibration from the reference to the working standard lamps for a calibration scheme similar to that of AAO has been estimated to ±2%. In our case, a significant contribution to the calibration transfer uncertainties comes from the statistical noise in the measurements which is different in different periods. Before 2018, the additional uncertainty in the Level 2 responses due to the calibration transfer is 0.4% for all wavelengths. After begin using the new calibration system in 2018
690 (200 Watt lamp PFC with the extender and 1000 Watt lamps in the laboratory) the uncertainty increases to 0.7% and 0.6% at 300 nm and above 310 nm respectively.

5.1.3 Instability

The instability of the instrument can be attributed to a number of factors (some of which have been discussed in Sect. 3.7). In the period which mediates between two consecutive calibrations, the Level 2 response does not change by more than 1.5%,
695 unless something in the system setup has been changed. Assuming a rectangular probability we estimate that the relative uncertainty is 0.4%, which is in agreement with the results of Diémoz et al. (2011).

5.1.4 Heating of the diffuser

All experiments described in Sect. 3.5 resulted that the remaining error after correcting measurements for the effect of temperature is less than 0.5%. Furthermore, the temperature of the whole surface of the Teflon diffuser is homogeneous
700 within 2°C during lamp measurements which cannot justify errors larger than 0.2%. Assuming again a rectangular probability we estimate that the relative standard uncertainty is equal to 0.2%.

5.1.5 Non-linearity

The Bentham5541 does not seemingly suffer from non-linearity and even possible undetected, long-term effects would be already taken into account in the instrument instability (Sect. 5.1.3). Thus the relative uncertainty is zero.

705 ### 5.1.6 Lamp aging

Analysis of the record of the lamp irradiances showed that the 200 Watt lamps are stable within ±1% over the years, and after a certain point they begin drifting. The drift was never found to be larger than 2% for the period of one year which mediates between two consecutive calibrations of each lamp, either at the facilities of PMOD-WRC, or at AAO. Based on

the above we estimate that the relative standard uncertainty is again the same with that reported in Diémoz et al. (2011), i.e.
710   0.5%.

5.1.7 Lamp current and wavelength stability

As has been discussed in Gröbner and Sperfeld (2005), instabilities in the lamp current and the wavelength scale of the instrument may also affect the calibration. The corresponding standard uncertainties are in both cases estimated to 0.1%.

5.1.8 Statistic noise

715   For the period before 2018 the uncertainty due to the statistic noise of the measurements is that reported in Diémoz et al. (2011), i.e. ±0.2% at 300 nm and 0.1% at longer wavelengths. However, since July 2018, 1000 Watt FEL lamps are used as reference for the calibration of the 200 Watt lamps at AAO. The signal of the 1000 Watt lamps is lower relative to the signal of the 200 Watt lamps with the short calibrator setup resulting to higher noise. Furthermore, the distance between the sensor and the 200 Watt lamps during calibration has been increased (the long calibrator setup is currently used) resulting again to
720   lower signal, and more noise. Thus, the corresponding uncertainties are estimated to 0.6% and 0.4%.

5.1.9 Other sources of uncertainty

The results of the 2017 inter-comparison with QASUME, as well as characterization in the new optical laboratory in 2018 clearly showed that the lamp irradiances used since 2016 were not accurate and had to change. As discussed in Sect. 4.2.4 we estimated that the problem started when the lamps returned from Davos in 2016. Although the correction has been
725   applied from the specific time point and on, it was not possible to independently prove and certify that the problem did not start earlier or later. Thus, it is still possible that the calibration factor may be systematically over- or under-estimated in part of the period between the inter-comparisons of 2015 and 2017. Additional uncertainty of 1.6% has been added to the overall uncertainty of the calibration factor for the particular period.

5.1.10 Overall radiometric uncertainties

730   Based on the above discussion we consider that the uncertainty in the irradiance of the lamps used for the calibration differs significantly between the periods 24/07/2006 – 17/04/2011 and 18/04/2011 - present. During the former period the standard uncertainty is considered 2.3% for all wavelengths. In the latter period the uncertainty depends on lamp and wavelength. Thus, a strict calculation of the uncertainty would demand to take into account the uncertainties of the lamps used for each calibration and consider different uncertainty budget for each period between consecutive calibrations. However, for
735   simplicity we consider that for the particular period the uncertainty in the lamps' irradiance is equal to the maximum reported uncertainty in all certificates and wavelength depended (decreasing from 1.4% at 300 nm to 0.7% at 500 nm). This way we may slightly overestimate the overall radiometric uncertainty for particular periods (by up to 0.5% at 300 nm and

0.2% at 500 nm). The results of the analysis discussed in this section are summarized in Table 1, where the overall radiometric uncertainty for different periods is presented.

740

Table 1: Contribution of different sources in the overall radiometric uncertainty (in %) o the Level 2 AAO spectra.

Period	24/07/2006 – 17/04/2011			18/04/2011 – 16/06/2015			17/06/2015 – 24/09/2017			25/09/2017 – 17/07/2018			18/07/2018 – present		
Wavelength (nm) contribution	300	310 - 400	400 - 500	300	310 - 400	400 - 500	300	310 - 400	400 - 500	300	310 - 400	400 - 500	300	310 - 400	400 - 500
Lamp irradiance	2.3	2.3	2.3	1.4	1.1	0.7	1.4	1.1	0.7	1.4	1.1	0.7	1.4	1.1	0.7
Calibration transfer	0.4	0.4	0.4	0.4	0.4	0.4	0.4	0.4	0.4	0.4	0.4	0.4	0.7	0.6	0.6
Instability	0.4	0.4	0.4	0.4	0.4	0.4	0.4	0.4	0.4	0.4	0.4	0.4	0.4	0.4	0.4
Heating of the diffuser	0.2	0.2	0.2	0.2	0.2	0.2	0.2	0.2	0.2	0.2	0.2	0.2	0.2	0.2	0.2
Lamp aging	0.5	0.5	0.5	0.5	0.5	0.5	0.5	0.5	0.5	0.5	0.5	0.5	0.5	0.5	0.5
Lamp current	0.1	0.1	0.1	0.1	0.1	0.1	0.1	0.1	0.1	0.1	0.1	0.1	0.1	0.1	0.1
Wavelength stability	0.1	0.1	0.1	0.1	0.1	0.1	0.1	0.1	0.1	0.1	0.1	0.1	0.1	0.1	0.1
Statistical noise	0.2	0.1	0.1	0.2	0.1	0.1	0.2	0.1	0.1	0.2	0.1	0.1	0.6	0.4	0.4
Standard uncertainty	**2.4**	**2.4**	**2.4**	**1.6**	**1.4**	**1.1**	**2.3**	**2.1**	**1.9**	**1.6**	**1.4**	**1.1**	**1.8**	**1.5**	**1.2**
Expanded uncertainty	4.9	4.9	4.9	3.2	2.7	2.1	4.6	4.2	3.8	3.2	2.7	2.1	3.6	3.0	2.4

5.2 Overall measurement uncertainties

Although radiometric uncertainties play a major role in the formulation of the overall uncertainty budget, some more uncertainty sources in actual solar measurements also have a significant contribution. The most important are discussed in
745 the following sections.

5.2.1 Diffuser temperature

The uncertainty calculated in Sect. 5.1.4 is also representative for the field measurements. Thus, the standard uncertainty in the field spectral measurements is also 0.2%.

5.2.2 Linearity

750 Since 24 July 2006, the relative uncertainty is 0% as discussed in Sect. 5.1.5.

5.2.3 Cosine and azimuth response

Based on the results of Sect. 3.2 we estimate the following uncertainties due to the imperfect cosine response of the instrument.

For SZA below 70°: 0.3% in the UV-B, 0.6% in the UV-A, and 0.7% in the VIS

755   For SZA above 70°: 0.1% in the UV-B, 0.6% in the UV-A, and 1.2% in the VIS

These uncertainties correspond to Aosta altitude and atmospheric conditions for the Level 2 products.

Inhomogeneities in the azimuth response of the diffuser generally have a negligible contribution in the uncertainty budget of the measurements. As discussed in Sect. 3.3, there are however periods, during which mis-levelling of the diffuser or improper positioning of the fiber optic in the OH induce more significant uncertainties. In these periods, the relative standard

760   uncertainty may be up to 2%.

5.2.4 Other uncertainty sources

Other sources of uncertainty which have been already discussed in previous studies are the statistic noise and the wavelength misalignment of the instrument. Both are more significant for short wavelengths and large SZAs (4.6% and 2.4% respectively at 300 nm for SZA=75°) and less significant for larger wavelengths and smaller SZAs (below 0.3% and 0.9%

765   respectively for wavelengths longer than 400 nm and SZA below 50°). The contribution of these sources has been already discussed in Diémoz et al. (2011).

5.2.5 Overall uncertainty budget

The overall uncertainty budget for different periods has been calculated by taking into account the same factors as Diémoz et al. (2011). The results for different periods are presented in Table 2.

770   **Table 2. Standard uncertainty in the spectral measurements of the Bentham5541 for different periods. The series for Level 2 spectra stops in July 2019 when the last QASUME intercomparison took place.**

Period	300nm SZA<50°	300nm SZA<75°	310–400nm SZA<50°	310–400nm SZA<75°	400–500nm SZA<50°	400–500nm SZA<75°
24/07/2006–20/12/2006	3.9	6.1	3.3	3.5	3.0	3.2
21/12/2006 – 17/04/2011	3.3	5.7	2.7	2.8	2.7	3.0
18/04/2011 – 26/08/2011	2.8	5.4	1.8	2.0	1.7	2.1
27/08/2011 – 07/07/2014	3.0	5.5	2.1	2.3	2.6	2.9
08/07/2014 – 13/01/2015	2.8	5.4	1.9	2.1	1.7	2.2
14/01/2015 – 16/06/2015	2.8	5.4	1.8	2.0	1.7	2.1
17/06/2015 –	3.3	5.7	2.4	2.6	2.3	2.6

24/09/2017						
25/09/2017 – 17/07/2018	2.8	5.4	1.8	2.0	1.7	2.1
18/07/2018 – 08/07/2019	2.9	5.5	1.9	2.1	1.7	2.2

It can be perceived from Table 2 that for the full time series and for SZAs below 75° the standard uncertainty at 300 nm is 6% or smaller, while for wavelengths in the UV-A and VIS it is below 3.5%.

775   The uncertainties in the erythemal and total UV-A irradiances (calculated from the spectra measured by the AAO) have been also quantified, assuming that uncertainties due to wavelength misalignment are negligible. For SZA below 75° the standard uncertainty in erythemal irradiance is of the order of 5% before 17/04/2011 and 4% thereafter. The corresponding uncertainties in UV-A are 3% and 2% respectively.

6 Summary and future prospects

780   The network of the Aosta Valley has been the first UV monitoring network in Italy. The reference instrument of the network is a Bentham DTMc300 spectrometer which has been performing automated continuous spectral scans of the solar irradiance in the range 290 – 500 nm since 2006, and is used as the reference instrument for all broadband instruments of the network. A rigorous QA/QC protocol and a strong traceability chain ensure the good quality of the spectra recorded by the Bentham5541. In the present study the methodology used to characterize the instrument for its individual characteristics, 785   correct the measurements, and quantify the relative uncertainties is described. Recently, the whole dataset has been re-evaluated and a new, highly accurate UV dataset has been produced.

In addition to the re-evaluation of the whole record of calibration factors, the accuracy of the Level 2 spectra has been improved significantly relative to the Level 1 spectra after applying a correction for the effect of temperature on the transmissivity of the Teflon diffuser. The accuracy of the correction for this effect has been proved through different 790   experiments. It has been also proved that the response of the instrument is linear, even for very high signal levels. In 2006, the HV of the PMT was set to a very low level (~ 400V) relative to the HV of other similar instruments (usually above 600V). Although the decrease in HV led to a large decrease in the response, thus a lower signal to noise ratio, it also eliminated the significant non-linearity issues which existed before the mid of 2006. In the near future there will be an effort to determine an optimal level of the HV for which the signal to noise ratio will increase without introducing non-linearity.

795   Uncertainties related to the calibration of the instrument have significant contribution to the overall uncertainty budget. Improved characterization (by PMOD-WRC) of the lamps used for the calibration of the AAO after 2011 led to more accurate determination of their irradiances and a reduction of the overall standard uncertainty in the measurements by ~1%. For wavelengths above 310 nm and SZAs below 75° the uncertainty in the former period is ~3%, while in the latter it is ~2%. At 300 nm the uncertainties are 5 – 6% and are dominated by uncertainties due the statistical noise and wavelength 800   instability. The overall uncertainty budget varies through the years, mainly as a result of different problems that affected the

measurements during different periods. Further reduction in the overall uncertainty budget is expected in the future due to the planned replacement of the currently used Teflon diffuser by a new diffuser with improved angular response. This study clearly points out the necessity of a maintaining a strong traceability chain to a reference instruments, in addition to keeping a strict QA/QC protocol. This way it is possible to detect dis-continuities and errors in the time-series which might induce

805   significant biases in the study of the trends of the spectral solar UV irradiance.

The new, low uncertainty Level 2 dataset is suitable for climatological studies and validation UV retrievals from satellite measurements and models. The time-series of the noon UV index as it has been calculated from the spectra is presented in Figure 9.
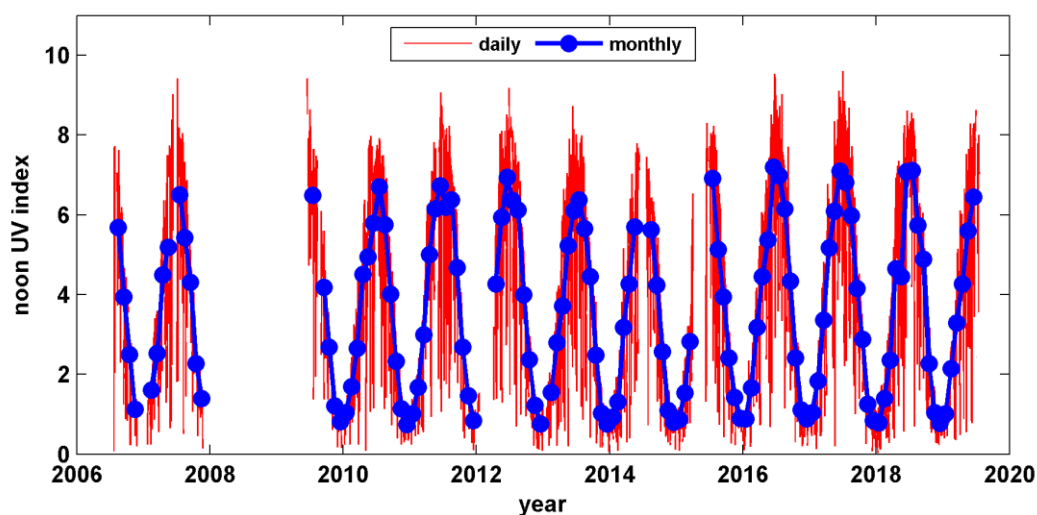
810   **Figure 9: The daily and monthly average noon UV index for the period 2006 – 2019, for which Level 2 data are available.**

The noon UV index for each day has been calculated as the average of available measurements for ±15 minutes around the exact local noon. The monthly averages have been calculated when at the UV index for at least 15 days of the month is available. The UV index in Aosta-Saint Christophe ranges from very low values (near zero) in winter and under cloudy conditions to very high values of ~9 in summer. Monthly averages range from 1 in winter to 6 or 7 in summer months. The

815   large variability of the daily and monthly UV index is indicative for the need of continuous UV monitoring. Further climatological analysis is however out of the scope of the present study and will be addressed in an upcoming article.

7 Data availability

The new Level 2 spectral UV dataset is freely available at https://doi.org/10.5281/zenodo.3934324 (Fountoulakis et al., 2020). The noon UV index used to create Fig. 9 is also available at the same repository. Analytical information regarding the

820   format and the context of the provided files can be found in the accompanying readme.txt file. The provided files are in csv format and include the spectra as well as the time of the beginning and the end of each scan. The NetCDF stored in the

database (see Sect. 4.2.5) have not been directly uploaded since they contain a very large amount of information which is not useful to the end user. However they are freely available and can be provided by the station PI (Henri Diémoz, e-mail: h.diemoz@arpa.vda.it). In case of any publication involving the particular dataset, co-authorship should be considered if the dataset plays a substantial role in the study. Acknowledgement of the dataset should be in all cases determined in consultation with the station PI. It is planned that the Level 2 spectra will also be submitted to the WOUDC (https://woudc.org/) and the European UV database (EUVDB) (http://uv.fmi.fi/uvdb/) (Heikkilä et al., 2016) in due course.

References

Anderson, G. P.: AFGL Atmospheric Constituent Profiles (0-120km), Optical Physics Division, Air Force Geophysics Laboratory, 1986.

Antón, M., Serrano, A., Cancillo, M. L., Vilaplana, J., Cachorro, V. E., and Gröbner, J.: Correction of Angular Response Error in Brewer UV Irradiance Measurements, Journal of Atmospheric and Oceanic Technology, 25, 2018-2027, 10.1175/2008jtecha1040.1, 2008.

Bais, A. F.: Spectrometers: Operational Errors and Uncertainties, Solar Ultraviolet Radiation, Berlin, Heidelberg, 1997, 165-173,

Bais, A. F., Kazadzis, S., Balis, D., Zerefos, C. S., and Blumthaler, M.: Correcting global solar ultraviolet spectra recorded by a Brewer spectroradiometer for its angular response error, Appl. Opt., 37, 6339-6344, 10.1364/ao.37.006339, 1998.

Bais, A. F., Gardiner, B. G., Slaper, H., Blumthaler, M., Bernhard, G., McKenzie, R., Webb, A. R., Seckmeyer, G., Kjeldstad, B., Koskela, T., Kirsch, P. J., Gröbner, J., Kerr, J. B., Kazadzis, S., Leszczynski, K., Wardle, D., Josefsson, W., Brogniez, C., Gillotay, D., Reinen, H., Weihs, P., Svenoe, T., Eriksen, P., Kuik, F., and Redondas, A.: SUSPEN intercomparison of ultraviolet spectroradiometers, Journal of Geophysical Research: Atmospheres, 106, 12509-12525, 10.1029/2000jd900561, 2001.

Bais, A. F., McKenzie, R. L., Bernhard, G., Aucamp, P. J., Ilyas, M., Madronich, S., and Tourpali, K.: Ozone depletion and climate change: impacts on UV radiation, Photochemical & Photobiological Sciences, 14, 19-52, 10.1039/c4pp90032d, 2015.

Bernhard, G., and Seckmeyer, G.: Uncertainty of measurements of spectral solar UV irradiance, Journal of Geophysical Research: Atmospheres, 104, 14321-14345, 10.1029/1999jd900180, 1999.

Bernhard, G., Booth, C. R., and McPeters, R. D.: Calculation of total column ozone from global UV spectra at high latitudes, Journal of Geophysical Research: Atmospheres, 108, 10.1029/2003jd003450, 2003.

Bernhard, G.: Trends of solar ultraviolet irradiance at Barrow, Alaska, and the effect of measurement uncertainties on trend detection, Atmos. Chem. Phys., 11, 13029-13045, 10.5194/acp-11-13029-2011, 2011.

Bernhard, G., and Petkov, B.: Measurements of spectral irradiance during the solar eclipse of 21 August 2017: reassessment of the effect of solar limb darkening and of changes in total ozone, Atmos. Chem. Phys., 19, 4703-4719, 10.5194/acp-19-4703-2019, 2019.

BIPM, IEC, IFCC, ILAC, ISO, IUPAC, IUPAP, and OIML: Evaluation of Measurement Data-Guide to the Expression of Uncertainty in Measurement GUM 1995 with minor corrections, Joint Committee for Guides in Metrology. 2008.

Blumthaler, M.: UV Monitoring for Public Health, International Journal of Environmental Research and Public Health, 15, 10.3390/ijerph15081723, 2018.

860 Booth, C. R., Lucas, T. B., Morrow, J. H., Weiler, C. S., and Penhale, P. A.: The United States National Science Foundation's Polar Network for Monitoring Ultraviolet Radiation, in: Ultraviolet Radiation in Antarctica: Measurements and Biological Effects, 17-37, 2013.

Bornman, J. F., Barnes, P. W., Robson, T. M., Robinson, S. A., Jansen, M. A. K., Ballaré, C. L., and Flint, S. D.: Linkages between stratospheric ozone, UV radiation and climate change and their implications for terrestrial ecosystems, Photochemical & Photobiological Sciences, 18, 681-716, 10.1039/c8pp90061b, 2019.

865 Bouillon, R., Eisman, J., Garabedian, M., Holick, M., Kleinschmidt, J., Suda, T., Terenetskaya, I., and Webb, A.: Action spectrum for the production of previtamin D3 in human skin, CIE, 174, 1-12, 2006.

Cadario, F., Savastio, S., Magnani, C., Cena, T., Pagliardini, V., Bellomo, G., Bagnati, M., Vidali, M., Pozzi, E., Pamparana, S., Zaffaroni, M., Genoni, G., and Bona, G.: High Prevalence of Vitamin D Deficiency in Native versus Migrant Mothers and Newborns in the North of Italy: A Call to Act with a Stronger Prevention Program, PLOS ONE, 10, e0129586, 870 10.1371/journal.pone.0129586, 2015.

Caldwell, M. M.: Solar ultraviolet radiation and the growth and development of higher plants, in: Photophysiology: Current Topics in Photobiology and Photochemistry, 6, Academic Press, New York, 131 - 177, 1971.

Caldwell, M. M., Björn, L. O., Bornman, J. F., Flint, S. D., Kulandaivelu, G., Teramura, A. H., and Tevini, M.: Effects of increased solar ultraviolet radiation on terrestrial ecosystems, Journal of Photochemistry and Photobiology B: Biology, 46, 875 40-52, https://doi.org/10.1016/S1011-1344(98)00184-5, 1998.

Casale, G. R., Siani, A. M., Diémoz, H., Agnesod, G., Parisi, A. V., and Colosimo, A.: Extreme UV index and solar exposures at Plateau Rosà (3500ma.s.l.) in Valle d'Aosta Region, Italy, Science of The Total Environment, 512-513, 622-630, https://doi.org/10.1016/j.scitotenv.2015.01.049, 2015.

CIE: CIE S007/E-1998 Erythema reference action spectrum and standard erythema dose, Color Research & Application, 24, 880 158-158, 10.1002/(sici)1520-6378(199904)24:2<158::aid-col11>3.0.co;2-4, 1999.

Cordero, R. R., Seckmeyer, G., Pissulla, D., DaSilva, L., and Labbe, F.: Uncertainty evaluation of spectral UV irradiance measurements, Measurement Science and Technology, 19, 045104, 10.1088/0957-0233/19/4/045104, 2008.

De Mazière, M., Thompson, A. M., Kurylo, M. J., Wild, J. D., Bernhard, G., Blumenstock, T., Braathen, G. O., Hannigan, J. W., Lambert, J. C., Leblanc, T., McGee, T. J., Nedoluha, G., Petropavlovskikh, I., Seckmeyer, G., Simon, P. C., Steinbrecht, 885 W., and Strahan, S. E.: The Network for the Detection of Atmospheric Composition Change (NDACC): history, status and perspectives, Atmos. Chem. Phys., 18, 4935-4964, 10.5194/acp-18-4935-2018, 2018.

Diémoz, H., and Mayer, B.: UV radiation in a mountaineous terrain: comparison of accurate 3D and fast 1D calculations in terms of UV index, One century of UV radiation research, Davos, Switzerland, 18 – 20 Sept 2007, 2007.

Diémoz, H., Siani, A. M., Casale, G. R., di Sarra, A., Serpillo, B., Petkov, B., Scaglione, S., Bonino, A., Facta, S., Fedele, F., 890 Grifoni, D., Verdi, L., and Zipoli, G.: First national intercomparison of solar ultraviolet radiometers in Italy, Atmos. Meas. Tech., 4, 1689-1703, 10.5194/amt-4-1689-2011, 2011.

Diémoz, H., Egli, L., Gröbner, J., Siani, A. M., and Diotri, F.: Solar ultraviolet irradiance measurements in Aosta (Italy): An analysis of short- and middle-term spectral variability, AIP Conference Proceedings, 1531, 856-859, 10.1063/1.4804905, 2013.

895   Diémoz, H., Campanelli, M., and Estellés, V.: One Year of Measurements with a POM-02 Sky Radiometer at an Alpine EuroSkyRad Station, Journal of the Meteorological Society of Japan. Ser. II, 92A, 1-16, 10.2151/jmsj.2014-A01, 2014.

Diémoz, H., Barnaba, F., Magri, T., Pession, G., Dionisi, D., Pittavino, S., Tombolato, I. K. F., Campanelli, M., Della Ceca, L. S., Hervo, M., Di Liberto, L., Ferrero, L., and Gobbi, G. P.: Transport of Po Valley aerosol pollution to the northwestern Alps – Part 1: Phenomenology, Atmos. Chem. Phys., 19, 3065-3095, 10.5194/acp-19-3065-2019, 2019a.

900   Diémoz, H., Gobbi, G. P., Magri, T., Pession, G., Pittavino, S., Tombolato, I. K. F., Campanelli, M., and Barnaba, F.: Transport of Po Valley aerosol pollution to the northwestern Alps – Part 2: Long-term impact on air quality, Atmos. Chem. Phys., 19, 10129-10160, 10.5194/acp-19-10129-2019, 2019b.

Eaton, B., Gregory, J., Drach, B., Taylor, K., Hankin, S., Blower, J., Caron, J., Signell, R., Bentley, P., Rappa, G., Höck, H., Pamment, A., Juckes, M., Raspaud, M., Horne, R., Whiteaker, T., Blodgett, D., Zender, C., and Lee, D.: NetCDF Climate
905   and Forecast (CF) Metadata Conventions. 2020.

Egli, L., Gröbner, J., Hülsen, G., Bachmann, L., Blumthaler, M., Dubard, J., Khazova, M., Kift, R., Hoogendijk, K., Serrano, A., Smedley, A., and Vilaplana, J. M.: Quality assessment of solar UV irradiance measured with array spectroradiometers, Atmos. Meas. Tech., 9, 1553-1567, 10.5194/amt-9-1553-2016, 2016.

Emde, C., Buras-Schnell, R., Kylling, A., Mayer, B., Gasteiger, J., Hamann, U., Kylling, J., Richter, B., Pause, C., Dowling, 910   T., and Bugliaro, L.: The libRadtran software package for radiative transfer calculations (version 2.0.1), Geosci. Model Dev., 9, 1647-1672, 10.5194/gmd-9-1647-2016, 2016.

Fountoulakis, I., Redondas, A., Bais, A. F., Rodriguez-Franco, J. J., Fragkos, K., and Cede, A.: Dead time effect on the Brewer measurements: correction and estimated uncertainties, Atmos. Meas. Tech., 9, 1799-1816, 10.5194/amt-9-1799-2016, 2016.

915   Fountoulakis, I., Redondas, A., Lakkala, K., Berjon, A., Bais, A. F., Doppler, L., Feister, U., Heikkila, A., Karppinen, T., Karhu, J. M., Koskela, T., Garane, K., Fragkos, K., and Savastiouk, V.: Temperature dependence of the Brewer global UV measurements, Atmos. Meas. Tech., 10, 4491-4505, 10.5194/amt-10-4491-2017, 2017.

Fountoulakis, I., Diémoz, H., Siani, A.-M., Laschewski, G., Filippa, G., Arola, A., Bais, A. F., De Backer, H., Lakkala, K., Webb, A. R., De Bock, V., Karppinen, T., Garane, K., Kapsomenakis, J., Koukouli, M.-E., and Zerefos, C. S.: Solar UV 920   Irradiance in a Changing Climate: Trends in Europe and the Significance of Spectral Monitoring in Italy, Environments, 7, 10.3390/environments7010001, 2019.

Fountoulakis, I., Diémoz, H., Siani, A. M., Hülsen, G., and Gröbner, J.: Level 2 spectra of the global solar irradiance in the wavelength range 290 - 500 nm measured at Aosta - Saint Christophe, Italy by the Bentham DTMc300 with serial number 5541 in 2006 - 2019, doi:10.5281/zenodo.3934324, 2020. In: zenodo, 2020.

925   Garane, K., Bais, A. F., Kazadzis, S., Kazantzidis, A., and Meleti, C.: Monitoring of UV spectral irradiance at Thessaloniki (1990–2005): data re-evaluation and quality control, Ann. Geophys., 24, 3215-3228, 10.5194/angeo-24-3215-2006, 2006.

Glandorf, M., Arola, A., Bais, A., and Seckmeyer, G.: Possibilities to detect trends in spectral UV irradiance, Theoretical and Applied Climatology, 81, 33-44, 10.1007/s00704-004-0109-9, 2005.

930   Gröbner, J., Blumthaler, M., and Ambach, W.: Experimental investigation of spectral global irradiance measurement errors due to a non ideal cosine response, Geophysical Research Letters, 23, 2493-2496, 10.1029/96gl02380, 1996.

Gröbner, J.: Improved entrance optic for global irradiance measurements with a Brewer spectrophotometer, Appl. Opt., 42, 3516 - 3521, 10.1364/AO.42.003516, 2003.

Gröbner, J., Schreder, J., Kazadzis, S., Bais, A. F., Blumthaler, M., Görts, P., Tax, R., Koskela, T., Seckmeyer, G., Webb, A. R., and Rembges, D.: Traveling reference spectroradiometer for routine quality assurance of spectral solar ultraviolet irradiance measurements, Appl. Opt., 44, 5321-5331, 10.1364/ao.44.005321, 2005.

Gröbner, J., and Sperfeld, P.: Direct traceability of the portable QASUME irradiance scale to the primary irradiance standard of the PTB, Metrologia, 42, 134-139, 10.1088/0026-1394/42/2/008, 2005.

Gröbner, J., Blumthaler, M., Kazadzis, S., Bais, A., Webb, A., Schreder, J., Seckmeyer, G., and Rembges, D.: Quality assurance of spectral solar UV measurements: results from 25 UV monitoring sites in Europe, 2002 to 2004, Metrologia, 43, S66-S71, 10.1088/0026-1394/43/2/s14, 2006.

Gröbner, J., and Blumthaler, M.: Experimental determination of the reference plane of shaped diffusers by solar ultraviolet measurements, Optics Letters, 32, 80-82, 10.1364/OL.32.000080, 2007.

Gröbner, J., Hülsen, G., Wuttke, S., Schrems, O., De Simone, S., Gallo, V., Rafanelli, C., Petkov, B., Vitale, V., Edvardsen, K., and Stebel, K.: Quality assurance of solar UV irradiance in the Arctic, Photochemical & Photobiological Sciences, 9, 384-391, 10.1039/b9pp00170k, 2010.

Häder, D. P., Kumar, H. D., Smith, R. C., and Worrest, R. C.: Effects of solar UV radiation on aquatic ecosystems and interactions with climate change, Photochemical & Photobiological Sciences, 6, 267-285, 10.1039/b700020k, 2007.

Heikkilä, A., Kaurola, J., Lakkala, K., Karhu, J. M., Kyrö, E., Koskela, T., Engelsen, O., Slaper, H., and Seckmeyer, G.: European UV DataBase (EUVDB) as a repository and quality analyser for solar spectral UV irradiance monitored in Sodankylä, Geosci. Instrum. Method. Data Syst., 5, 333-345, 10.5194/gi-5-333-2016, 2016.

Herman, J. R., Bhartia, P. K., Ziemke, J., Ahmad, Z., and Larko, D.: UV-B increases (1979–1992) from decreases in total ozone, Geophysical Research Letters, 23, 2117-2120, 10.1029/96gl01958, 1996.

Hintzpeter, B., Scheidt-Nave, C., Müller, M. J., Schenk, L., and Mensink, G. B. M.: Higher Prevalence of Vitamin D Deficiency Is Associated with Immigrant Background among Children and Adolescents in Germany, The Journal of Nutrition, 138, 1482-1490, 10.1093/jn/138.8.1482, 2008.

Huelsen, G., Gröbner, J., Bais, A., Blumthaler, M., Diemoz, H., Bolsee, D., Diaz Rodríguez, A., Fountoulakis, I., Naranen, E., Schreder, J., Stefania, F., and Vilaplana Guerrero, J. M.: Second solar ultraviolet radiometer comparison campaign UVC-II, Metrologia, 2020.

Hülsen, G., Gröbner, J., Nevas, S., Sperfeld, P., Egli, L., Porrovecchio, G., and Smid, M.: Traceability of solar UV measurements using the Qasume reference spectroradiometer, Appl. Opt., 55, 7265 - 7275, 10.1364/AO.55.007265, 2016.

Jablonski, N. G., and Chaplin, G.: The evolution of human skin coloration, Journal of Human Evolution, 39, 57-106, https://doi.org/10.1006/jhev.2000.0403, 2000.

Juzeniene, A., Brekke, P., Dahlback, A., Andersson-Engels, S., Reichrath, J., Moan, K., Holick, M. F., Grant, W. B., and Moan, J.: Solar radiation and human health, Reports on Progress in Physics, 74, 066701, 10.1088/0034-4885/74/6/066701, 2011.

Juzeniene, A., and Moan, J.: Beneficial effects of UV radiation other than via vitamin D production, Dermato-Endocrinology, 4, 109-117, 10.4161/derm.20013, 2012.

Kazadzis, S., Bais, A., Kouremeti, N., Gerasopoulos, E., Garane, K., Blumthaler, M., Schallhart, B., and Cede, A.: Direct spectral measurements with a Brewer spectroradiometer: absolute calibration and aerosol optical depth retrieval, Appl. Opt., 44, 1681-1690, 10.1364/ao.44.001681, 2005.

Kerr, J. B., and McElroy, C. T.: Evidence for Large Upward Trends of Ultraviolet-B Radiation Linked to Ozone Depletion, Science, 262, 1032, 10.1126/science.262.5136.1032, 1993.

975 Lakkala, K., Arola, A., Heikkilä, A., Kaurola, J., Koskela, T., Kyrö, E., Lindfors, A., Meinander, O., Tanskanen, A., Gröbner, J., and Hülsen, G.: Quality assurance of the Brewer spectral UV measurements in Finland, Atmos. Chem. Phys., 8, 3369-3383, 10.5194/acp-8-3369-2008, 2008.

Lakkala, K., Arola, A., Gröbner, J., León-Luis, S. F., Redondas, A., Kazadzis, S., Karppinen, T., Karhu, J. M., Egli, L., Heikkilä, A., Koskela, T., Serrano, A., and Vilaplana, J. M.: Performance of the FMI cosine error correction method for the Brewer spectral UV measurements, Atmos. Meas. Tech., 11, 5167-5180, 10.5194/amt-11-5167-2018, 2018.

980 Lips, P., and de Jongh, R. T.: Vitamin D deficiency in immigrants, Bone Reports, 9, 37-41, https://doi.org/10.1016/j.bonr.2018.06.001, 2018.

Lucas, R. M., Yazar, S., Young, A. R., Norval, M., de Gruijl, F. R., Takizawa, Y., Rhodes, L. E., Sinclair, C. A., and Neale, R. E.: Human health in relation to exposure to solar ultraviolet radiation under changing stratospheric ozone and climate, Photochemical & Photobiological Sciences, 18, 641-680, 10.1039/c8pp90060d, 2019.

985 McKenzie, R. L., Kotkamp, M., Seckmeyer, G., Erb, R., Roy, C. R., Gies, H. P., and Toomey, S. J.: First southern hemisphere intercomparison of measured solar UV spectra, Geophysical Research Letters, 20, 2223-2226, 10.1029/93gl02359, 1993.

Petkov, B. H., Vitale, V., Tomasi, C., Siani, A. M., Seckmeyer, G., Webb, A. R., Smedley, A. R. D., Casale, G. R., Werner, R., Lanconelli, C., Mazzola, M., Lupi, A., Busetto, M., Diémoz, H., Goutail, F., Köhler, U., Mendeva, B. D., Josefsson, W., 990 Moore, D., Bartolomé, M. L., Moreta González, J. R., Mišaga, O., Dahlback, A., Tóth, Z., Varghese, S., De Backer, H., Stübi, R., and Vaníček, K.: Response of the ozone column over Europe to the 2011 Arctic ozone depletion event according to ground-based observations and assessment of the consequent variations in surface UV irradiance, Atmospheric Environment, 85, 169-178, https://doi.org/10.1016/j.atmosenv.2013.12.005, 2014.

Pulli, T., Kärhä, P., Mes, J., Schreder, J., Jaanson, P., and Manoocheri, F.: Improved diffusers for solar UV 995 spectroradiometers, AIP Conference Proceedings, 1531, 813-816, 10.1063/1.4804894, 2013.

Schmalwieser, A. W., Gröbner, J., Blumthaler, M., Klotz, B., De Backer, H., Bolsée, D., Werner, R., Tomsic, D., Metelka, L., Eriksen, P., Jepsen, N., Aun, M., Heikkilä, A., Duprat, T., Sandmann, H., Weiss, T., Bais, A., Toth, Z., Siani, A.-M., Vaccaro, L., Diémoz, H., Grifoni, D., Zipoli, G., Lorenzetto, G., Petkov, B. H., di Sarra, A. G., Massen, F., Yousif, C., Aculinin, A. A., den Outer, P., Svendby, T., Dahlback, A., Johnsen, B., Biszczuk-Jakubowska, J., Krzyscin, J., Henriques, 1000 D., Chubarova, N., Kolarž, P., Mijatovic, Z., Groselj, D., Pribullova, A., Gonzales, J. R. M., Bilbao, J., Guerrero, J. M. V., Serrano, A., Andersson, S., Vuilleumier, L., Webb, A., and O'Hagan, J.: UV Index monitoring in Europe, Photochemical & Photobiological Sciences, 16, 1349-1370, 10.1039/c7pp00178a, 2017.

Seckmeyer, G., Thiel, S., Blumthaler, M., Fabian, P., Gerber, S., Gugg-Helminger, A., Häder, D.-P., Huber, M., Kettner, C., Köhler, U., Köpke, P., Maier, H., Schäfer, J., Suppan, P., Tamm, E., and Thomalla, E.: Intercomparison of spectral-UV-1005 radiation measurement systems, Appl. Opt., 33, 7805 - 7812, 10.1364/AO.33.007805, 1994.

Seckmeyer, G., Smolskaia, I., Pissulla, D., Bais, A. F., Tourpali, K., Meleti, C., and Zerefos, C.: Solar UV: Measurements and Trends, Twenty Years of Ozone Decline, Dordrecht, 2009, 359-368,

Setlow, R. B.: The wavelengths in sunlight effective in producing skin cancer: a theoretical analysis, Proc Natl Acad Sci U S A, 71, 3363-3366, 10.1073/pnas.71.9.3363, 1974.

1010 Siani, A. M., Casale, G. R., Diémoz, H., Agnesod, G., Kimlin, M. G., Lang, C. A., and Colosimo, A.: Personal UV exposure in high albedo alpine sites, Atmos. Chem. Phys., 8, 3749-3760, 10.5194/acp-8-3749-2008, 2008.

Siani, A. M., Frasca, F., Scarlatti, F., Religi, A., Diémoz, H., Casale, G. R., Pedone, M., and Savastiouk, V.: Examination on total ozone column retrievals by Brewer spectrophotometry using different processing software, Atmos. Meas. Tech., 11, 5105-5123, 10.5194/amt-11-5105-2018, 2018.

1015   Slaper, H., Reinen, H. A. J. M., Blumthaler, M., Huber, M., and Kuik, F.: Comparing ground-level spectrally resolved solar UV measurements using various instruments: A technique resolving effects of wavelength shift and slit width, Geophysical Research Letters, 22, 2721-2724, doi:10.1029/95GL02824, 1995.

Solomon, S., Garcia, R. R., Rowland, F. S., and Wuebbles, D. J.: On the depletion of Antarctic ozone, Nature, 321, 755-758, 10.1038/321755a0, 1986.

1020   Weatherhead, E. C., Reinsel, G. C., Tiao, G. C., Meng, X.-L., Choi, D., Cheang, W.-K., Keller, T., DeLuisi, J., Wuebbles, D. J., Kerr, J. B., Miller, A. J., Oltmans, S. J., and Frederick, J. E.: Factors affecting the detection of trends: Statistical considerations and applications to environmental data, Journal of Geophysical Research: Atmospheres, 103, 17149-17161, 10.1029/98jd00995, 1998.

Webb, A. R., and Engelsen, O.: Ultraviolet Exposure Scenarios: Risks of Erythema from Recommendations on Cutaneous
1025   Vitamin D Synthesis, in: Sunlight, Vitamin D and Skin Cancer, edited by: Reichrath, J., Springer New York, New York, NY, 72-85, 2008.

Webb, A. R., Slaper, H., Koepke, P., and Schmalwieser, A. W.: Know Your Standard: Clarifying the CIE Erythema Action Spectrum, Photochemistry and Photobiology, 87, 483-486, 10.1111/j.1751-1097.2010.00871.x, 2011.

Ylianttila, L., and Schreder, J.: Temperature effects of PTFE diffusers, Optical Materials, 27, 1811-1814,
1030   https://doi.org/10.1016/j.optmat.2004.11.008, 2005.

Zerefos, C. S., Bais, A. F., Meleti, C., and Ziomas, I. C.: A note on the recent increase of Solar UV-B radiation over northern middle latitudes, Geophysical Research Letters, 22, 1245-1247, 10.1029/95gl01187, 1995.

Zuber, R., Ribnitzky, M., Tobar, M., Lange, K., Kutscher, D., Schrempf, M., Niedzwiedz, A., and Seckmeyer, G.: Global spectral irradiance array spectroradiometer validation according to WMO, Measurement Science and Technology, 29,
1035   105801, 10.1088/1361-6501/aada34, 2018.